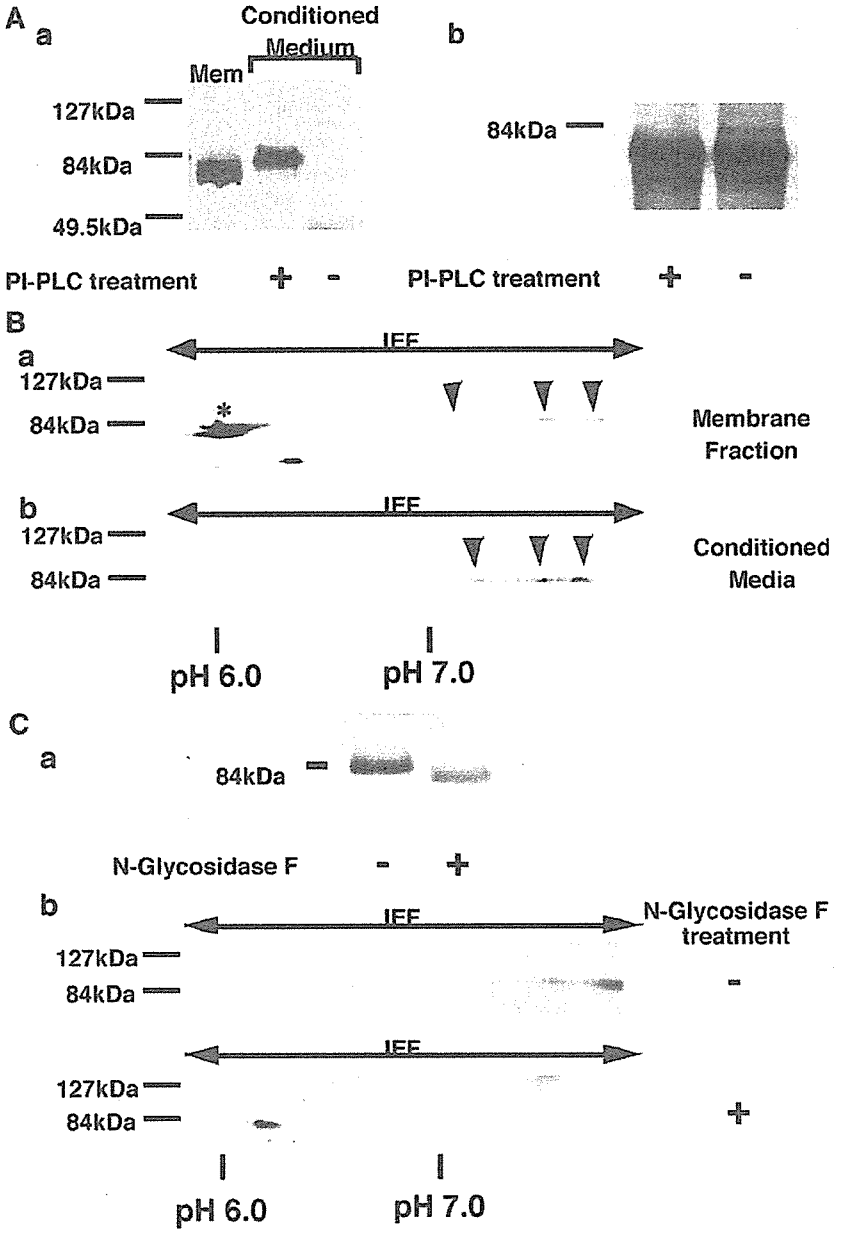

Fig. 1. Moesin-like protein is an 80 kDa HDL/apolipoprotein A-I (apoA-I) binding protein. A: Formation of moesin-like protein by phosphatidylinositol-specific phospholipase C (PI-PLC) treatment of human macrophages. After treatment of macrophages with or without 0.5 U/ml PI-PLC, the conditioned media were applied for immunoblotting analysis with anti-moesin antibody (TK88) (a). PI-PLC treatment resulted in the formation of the moesin-like protein from human macrophages. In control experiments (incubation without PI-PLC), no band was observed. After treatment with or without PI-PLC, the macrophage membranes were subjected to immunoblotting with anti-moesin antibody (b). The larger band of two moesin-like proteins was reduced after PI-PLC treatment. B: Two-dimensional immunoblotting using anti-moesin antibody. The membrane fraction of human macrophages (a) and the conditioned media after PI-PLC treatment with macrophages (b) were applied for two-dimensional immunoblotting analysis with anti-moesin antibody (TK88). A massive amount of moesin at pH 6.0 (asterisk), as predicted by the amino acid content of moesin, and a small amount of protein with an isoelectric point of pH 7.2 to 7.6 (arrowheads) were observed in membrane fraction proteins. The conditioned media with PI-PLC treatment showed moesin-like protein (arrowheads) but not moesin. C: Enzymatic deglycosylation of moesin-like protein with N-glycosidase F. The conditioned media, after treatment with 0.5 U/ml PI-PLC for 24 h at 37°C, were incubated with or without N-glycosidase F. After digestion with the enzyme, the treated or nontreated conditioned media were applied for immunoblotting with anti-moesin antibody (TK88). The immunoreactive protein of digested media was shifted down compared with that of nondigested media (a), and the isoelectric point of the protein (pH 7.2 to 7.6) changed to pH 6.0 (b), indicating that the protein was N-linked.

antibody were performed using flow cytometry (**Fig. 3A**). Compared with control IgG, anti-moesin monoclonal antibody reduced the MIF of FITC-labeled HDL3 from 46.0 to 21.9 (Fig. 3Aa) and that of FITC-labeled apoA-I from 203.2 to 80.0 (Fig. 3Ab). To confirm that anti-moesin antibody could specifically reduce HDL3 or apoA-I binding, we examined whether the antibody could suppress the bindings of DiI-oxidized LDL and DiI-AcLDL (Fig. 3Ac,

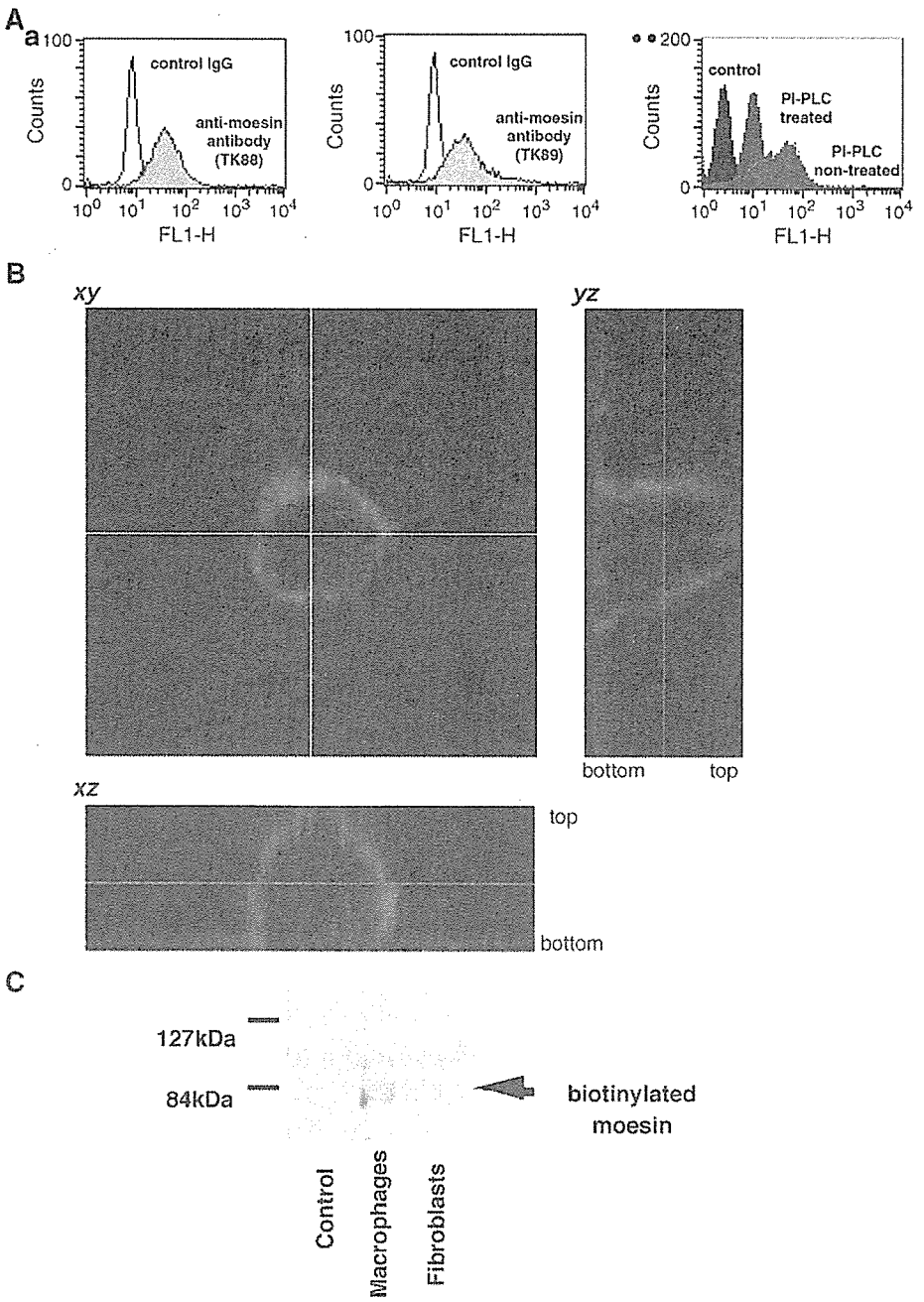

Fig. 2. Expression of moesin-like protein is on the cell surface of macrophages. A: Flow cytometric analyses of moesin-like protein on macrophages. After fixation with 4% paraformaldehyde, the lipid-laden macrophages were preincubated with 5% normal horse serum and then with control rabbit IgG or anti-moesin antibody (TK88 or TK89) (a). After washing, the cells were incubated with FITC-labeled goat anti-rabbit IgG antibody. Cell-bound fluorescence was detected by FACScan. After treatment with or without PI-PLC, the macrophages were applied for FACScan analyses with anti-moesin antibody (TK88) (b). PI-PLC treatment reduced the fluorescence of the moesin-like moiety. Red peak, PI-PLC nontreated macrophages; blue peak, PI-PLC-treated; black peak, control. B: Confocal microscopic analysis of moesin-like protein. For immunohistochemical analysis of moesin-like protein, cultured human macrophages were fixed with 4% paraformaldehyde, blocked with 5% normal horse serum, and then incubated with anti-moesin antibody (TK88) for 1 h, followed by sequential incubation with FITC-labeled anti-rabbit IgG antibody, and finally confocal microscopic analysis. Vertical sections (*xz* and *yz*) were projected. *En face* sections (*xy*) images were taken off the macrophage from the top to the bottom and computer-reconstructed vertical section (*xz* and *yz*) images were taken through the full thickness of the macrophage. C: Immunoprecipitation after cell surface biotinylation. The cultured macrophages and human fibroblasts were treated with NHS-biotin (water-soluble biotin) for 15 min at 4°C and then washed with 0.192 M glycine/25 mM Tris, pH 8.3, for 15 min at 4°C to quench the reaction. The membrane fractions were subjected to immunoprecipitation using anti-moesin antibody (TK88) and control IgG. Immunoprecipitates were applied for SDS-PAGE, transferred onto nitrocellulose membrane, and then visualized with streptavidin-horseradish peroxidase.

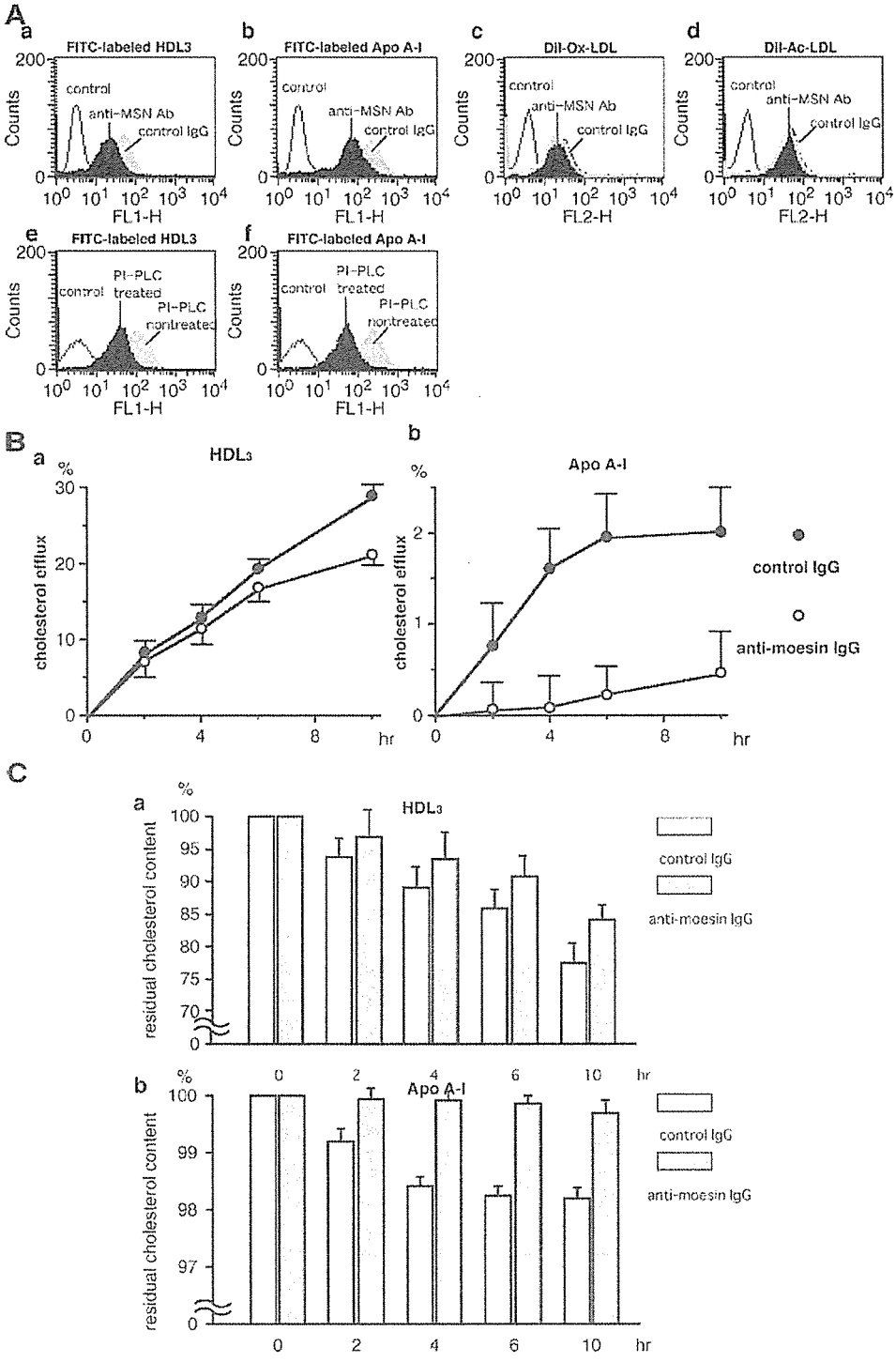

Fig. 3. Effects of anti-moesin antibody on HDL/apoA-I binding and HDL/apoA-I-mediated cholesterol efflux from macrophages. A: Flow cytometric analysis of HDL3/apoA-I-specific binding to macrophages via moesin-like protein. The effect of anti-moesin antibody on FITC-labeled HDL3 (a) and apoA-I (b) examined by flow cytometry. Anti-moesin antibody reduced the mean intensity of fluorescence (MIF), decreased HDL3 binding from 46.02 to 21.87, and apoA-I binding from 203.24 to 80.02. However, anti-moesin antibody did not affect DiI-labeled oxidized LDL (c) or DiI-labeled AcLDL (d). After PI-PLC treatment, binding studies were performed to determine the percentage of apoA-I (e) or HDL3 (f) binding due to this specific receptor. PI-PLC reduced the binding capacity of HDL3 by 67% and that of apoA-I by 76%. B: Anti-moesin antibody inhibits HDL3/apoA-I-mediated cholesterol efflux. Cholesterol efflux was evaluated as the transfer of [^{3}H]-labeled cholesterol from prelabeled macrophages to HDL3 (a) or apoA-I (b). The percentage of specific HDL3- or apoA-I-mediated cholesterol efflux was estimated by the difference between cholesterol efflux in the presence and absence of the ligands. Anti-moesin antibody decreased cholesterol efflux via HDL3 (a) and apoA-I (b) from macrophages throughout the experiment compared with the control IgG. C: Effect of anti-moesin antibody on residual cholesterol content in macrophages after HDL3 (a) or apoA-I (b) - mediated cholesterol efflux. Anti-moesin antibody suppressed the reduction of residual cholesterol after cholesterol efflux throughout the experiment. Data are mean ± SEM of n experiments.

Ad). Neither the distribution of DiI-oxidized LDL nor that of DiI-AcLDL-incorporated cells was affected by incubation with anti-moesin antibody. Next, to address the percentage of apoA-I or HDL binding due to this specific receptor, binding studies were performed using PI-PLC-treated cells (Fig. 3Ae and f). After treatment with PI-PLC, the binding capacity of HDL3 diminished from 121.5 to 39.5 (67% reduction) and that of apoA-I from 229.1 to 55.4 (76% reduction).

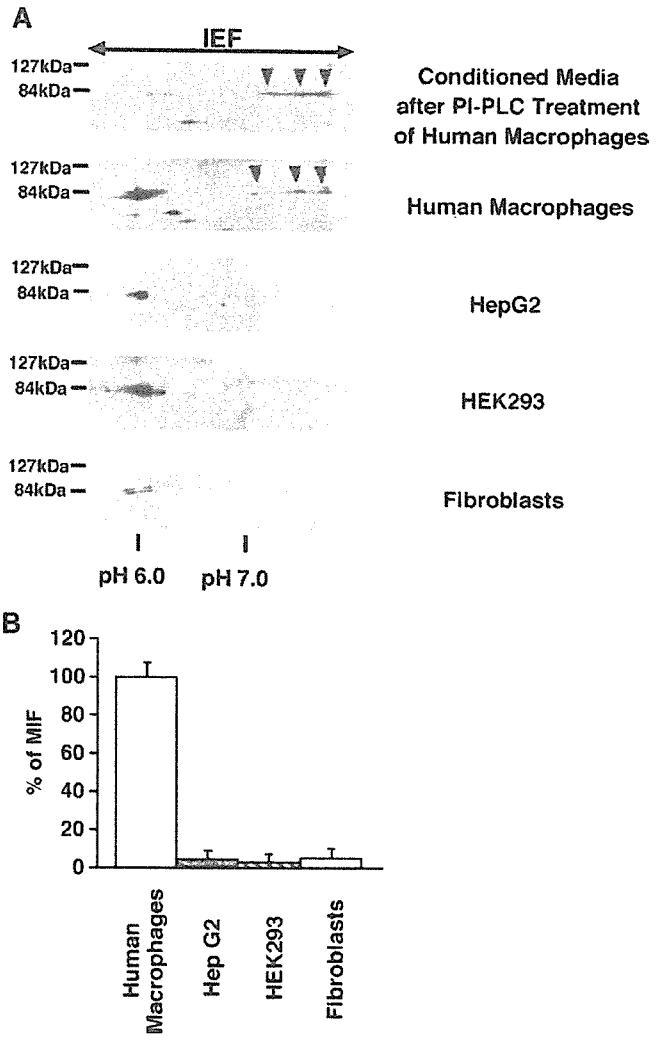

Fig. 4. Specific expression of the moesin-like protein on human macrophages. A: Cell lineage-specific expression of the moesin-like protein in two-dimensional immunoblotting. Membrane fractions derived from human macrophages, HepG2 cells, HEK293 cells, and human fibroblasts were subjected to two-dimensional immunoblotting analysis using anti-moesin antibody (TK88). Human macrophages expressed the moesin-like protein (arrowheads) in addition to moesin. Nonmonocyte-lineage cells (HepG2, HEK293, and human fibroblasts) expressed moesin but not moesin-like protein. B: Cell lineage-specific expression of the moesin-like protein by flow cytometry. Human macrophages, THP-1, HepG2 and HEK293 cells, and human fibroblasts were subjected to flow cytometry. The moesin-like protein was not detected in nonmonocyte-lineage cells (HepG2, HEK293, and human fibroblasts), but was expressed in human macrophages and THP-1 cells, suggesting that moesin-like protein is specifically expressed on monocyte-macrophages lineage. Data are mean ± SEM of n experiments. IEF, isoelectric focusing.

To confirm the physiological function of moesin-like protein on the cell surface, we next examined whether it was involved in the HDL/apoA-I-mediated cholesterol efflux from macrophages. As shown in Fig. 3B, treatment of macrophages with anti-moesin antibody reduced HDL- and apoA-I-mediated cholesterol efflux from macrophages throughout the experiment (up to 10 h). Next, we examined the effect of anti-moesin antibody on the residual cholesterol contents of macrophages after HDL- or apoA-I-mediated cholesterol efflux (Fig. 3C). Anti-moesin antibody lessened the reduction of residual cholesterol after cholesterol efflux. These results suggest that the moesin-like protein is involved in HDL- and apoA-I-mediated cholesterol efflux from human monocyte-derived macrophages.

Specific expression of moesin-like protein in monocytes/macrophages

To determine whether the cell surface-expressed moesin-like protein is specifically expressed on macrophages, two-dimensional immunoblotting was performed (**Fig. 4A**). Membrane fractions from human monocyte-derived macrophages, HepG2 cells, HEK293 cells, and human fibroblasts were collected and applied for two-dimensional immunoblotting with anti-moesin antibody (TK88). Human macrophages expressed moesin with an isoelectric point of pH 6.0 and moesin-like protein with an isoelectric point of pH 7.2 to 7.6. Cells other than monocyte macrophages expressed moesin (pH 6.0) but no moesin-like protein.

The moesin-like protein on the cell surface was further examined by flow cytometry, and its amount was determined as MIF in human macrophages, HepG2 cells, HEK293 cells, and human fibroblasts (Fig. 4B). The results confirmed the lack of moesin-like protein on the surface of nonmonocyte cell lines (HepG2, HEK293, and human fibroblasts) and its presence on human macrophages.

Effect of cholesterol loading and differentiation on the expression of moesin-like protein

To determine the functional role of the cell surface-expressed moesin-like protein in the reverse cholesterol transport system, we examined the effect of cholesterol loading. Six-day-cultured human macrophages were incubated for 24 h with or without AcLDL (50 μg/ml), and then subjected to flow cytometric analysis. The distribution of cell surface moesin-positive macrophages was shifted to the right by Ac-LDL loading (**Fig. 5Aa**), and the MIF of AcLDL-laden macrophages was upregulated about two-fold to that of unladen macrophages (Fig. 5Ab). To confirm that the moesin-like protein was increased after cholesterol loading, membrane fractions derived from Ac-LDL-laden and -unladen macrophages were applied for immunoblotting analyses using anti-moesin antibody (Fig. 5B). The larger band of two moesin-like proteins, which was shown as the cell surface-expressed moesin-like protein, was increased by cholesterol loading. These results suggest that the expression of cell surface-expressed moesin-like protein is enhanced in association with foam cell formation.

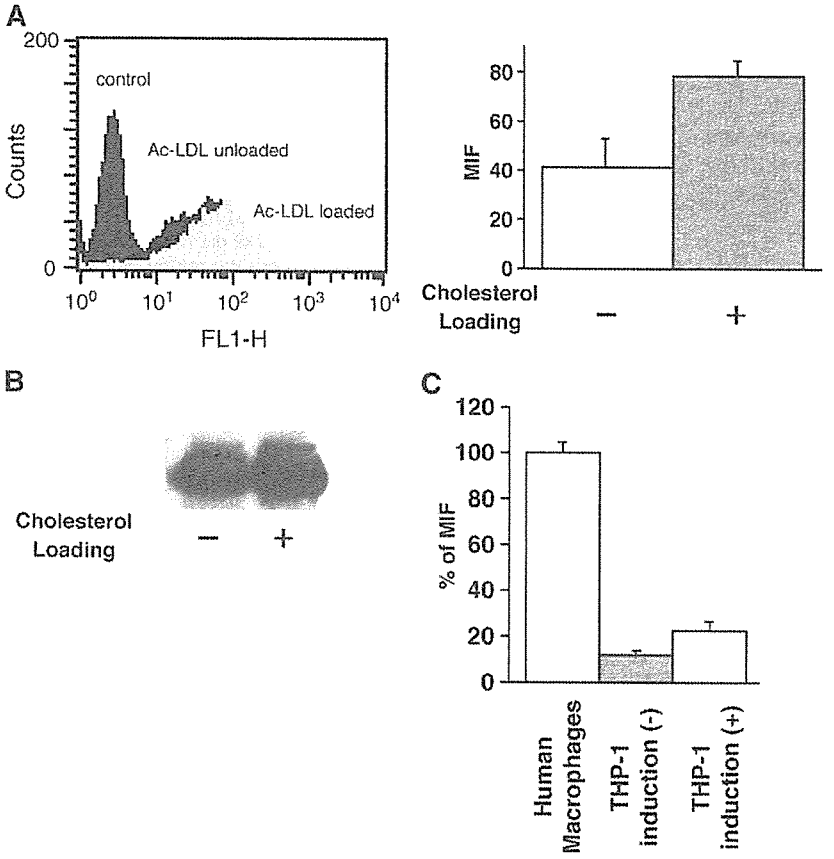

Fig. 5. A: Effect of cholesterol loading on moesin-like protein. Six day-cultured human macrophages were incubated for 24 h with or without AcLDL (50 μg/ml), and then subjected to flow cytometry. The MIF of AcLDL-laden macrophages was upregulated about two-fold relative to that of unladen macrophages. B: After loading cholesterol with Ac-LDL, the macrophage membranes were subjected to immunoblotting with anti-moesin antibody. The intensity of the larger band of two moesin-like proteins was increased on Ac-LDL-laden macrophages compared with nonladen. C: Effect of differentiation on moesin-like protein expression. THP-1 cells were treated with phorbol 12-myristate 13-acetate (PMA) (50 ng/ml) for 24 h and then subjected to flow cytometry. The MIF of the moesin-like protein after PMA treatment was double that before treatment. Data are mean ± SEM of n experiments.

Finally, we examined whether moesin-like protein increases with cell differentiation. For this purpose, THP-1 cells were treated with PMA and subjected to flow cytometric analysis (Fig. 5C). The MIF of moesin-like protein after PMA treatment was expressed twice as much as that before treatment, indicating that the cell surface-expressed moesin-like protein was upregulated with differentiation of monocytes into macrophages.

DISCUSSION

In the present study, we identified the protein recognized by anti-human moesin antibodies, and termed it moesin-like protein. The protein is a GPI-anchored type, is expressed on the cell surface of human macrophages, is induced by differentiation and cholesterol loading of macrophages, and is involved in the binding and cholesterol efflux of HDL/apoA-I.

Internal sequencing of the previously purified apoA-I/HDL binding protein matched the sequences of the two internal fragments of moesin. Moesin belongs to the ERM family of proteins (along with ezrin and radixin) that are known to be involved in cell adhesion and membrane dynamics, probably because of their ability to link plasma membrane components with the actin cytoskeleton (17–19). Although the functions of ERM proteins have not yet been fully delineated, these proteins are widely expressed in different tissues and cells. They have been identified in filopodia and are associated with other membranous proteins that are important for ligand recognition, signal transduction, and cell motility (17–20). Most previous reports have focused on moesin as a linking protein of the submembranous cytoskeleton.

Although moesin has a cell surface domain involved in the binding of lipopolysaccharides (21), IL-2 fragments (22), and human immunodeficiency virus type 1 envelope protein gp 120 (23), moesin has no signal peptide, is not expressed on the cell surface, and is not a GPI-anchored type protein. In this study, we demonstrated that the newly purified apoA-I/HDL binding protein is expressed on the cell surface, exclusively on macrophages, and is a GPI-anchored type. Two-dimensional immunoblotting analysis also revealed that the IEF of the protein (pH 7.2–7.6) is different from that of moesin (pH 6.0). We also showed that the protein underwent N-glycosylation. These characteristics are totally different from those of moesin, indicating that the protein is not moesin.

There are no reports on isoforms of moesin. The protein is recognized by two kinds of antibodies raised by human moesin. The epitopes of these antibodies are located between two internal sequences that matched the fragments sequences of the moesin-like protein. The RT-PCR product, with primers located on two matched sequences using RNAs from human macrophages, yielded a single band (data not shown). These data suggest that the protein prified in our study is an isoform of moesin. The isoform of moesin is thought to be transported by the Golgi-ER

pathway and expressed on the cell surface of human macrophages. Gelsolin, for example, also has two isoforms; one functions as an actin binding protein intracellularly, and the other has a signal peptide and is secreted by the liver. The pattern of expression is also different for the two gelsolin isoforms. This alternative splicing mechanism of gelsolin resembles that of moesin. One of two isoforms of moesin can be a cell surface binding site of HDL and apoA-I.

In conclusion, our data demonstrate that the cell surface-expressed moesin-like protein is a binding protein for apoA-I/HDL on the surface of human monocyte-derived macrophages and can stimulate apoA-I- /HDL-mediated cholesterol efflux. Further studies are in progress to clone the cell surface-expressed moesin-like protein, which may enhance our understanding of the initial step of reverse cholesterol transport.

This research was supported in part by grants-in-aid (10671067, 11557054, 11557055, and 12670666) from the Japanese Ministry of Education, Culture, Sports and Welfare; a grant from the Kanae Foundation; a grant from the Japan Heart Foundation/Pfizer for research on hypertension, hyperlipidemia, and vascular metabolism (A.M.); and an International HDL Research Awards Program grant (S.Y.) from Pfizer.

REFERENCES

1. Gordon, T., W. P. Castelli, M. C. Hjortland, W. B. Kannel, and T. R. Dawber. 1977. High density lipoprotein as a protective factor against coronary heart disease. The Framingham Study. *Am. J. Med.* **62:** 707–714.
2. Yamashita, S., N. Sakai, K. Hirano, T. Arai, M. Ishigami, T. Maruyama, and Y. Matsuzawa. 1997. Molecular genetics of plasma cholesteryl ester transfer protein. *Curr. Opin. Lipidol.* **8:** 101–110.
3. Oram, J. F., and S. Yokoyama. 1996. Apolipoprotein-mediated removal of cellular cholesterol and phospholipids. *J. Lipid Res.* **37:** 2473–2491.
4. Mendez, A. J., J. F. Oram, and E. L. Bierman. 1991. Protein kinase C as a mediator of high density lipoprotein receptor-dependent efflux of intracellular cholesterol. *J. Biol. Chem.* **266:** 10104–10111.
5. Matsumoto, A., A. Mitchell, H. Kurata, L. Pyle, K. Kondo, H. Itakura, and N. Fidge. 1997. Cloning and characterization of HB2, a candidate high density lipoprotein receptor. Sequence homology with members of the immunoglobulin superfamily of membrane proteins. *J. Biol. Chem.* **272:** 16778–16782.
6. Acton, S., A. Rigotti, K. T. Landschulz, S. Xu, H. H. Hobbs, and M. Krieger. 1996. Identification of scavenger receptor SR-BI as a high density lipoprotein receptor. *Science.* **271:** 518–520.
7. Ji, Y., B. Jian, N. Wang, Yu Sun, M. L. Moya, M. C. Phillips, G. H. Rothblat, J. B. Swaney, and A. R. Tall. 1997. Scavenger receptor BI promotes high density lipoprotein-mediated cellular cholesterol efflux. *J. Biol. Chem.* **272:** 20982–20985.
8. Hirano, K., S. Yamashita, Y. Nakagawa, T. Ohya, F. Matsuura, K. Tsukamoto, Y. Okamoto, A. Matsuyama, K. Matsumoto, J. Miyagawa, et al. 1999. Expression of human scavenger receptor class B type I in cultured human monocyte-derived macrophages and atherosclerotic lesions. *Circ. Res.* **85:** 108–116.
9. Wang, N., D. L. Silver, P. Costet, and A. R. Tall. 2000. Specific binding of Apo A-I, enhanced cholesterol efflux, and altered plasma membrane morphology in cells expressing ABC1. *J. Biol. Chem.* **275:** 33053–33058.
10. Hirano, K., F. Matsuura, K. Tsukamoto, Z. Z. Zhang, A. Matsuyama, K. Takaishi, R. Komuro, T. Suehiro, S. Yamashita, and Y. Takai. 2000. Decreased expression of a member of the Rho GTPase family, Cdc42Hs, in cells from Tangier disease - the small G protein may play a role in cholesterol efflux. *FEBS Lett.* **484:** 275–279.
11. Matsuyama, A., S. Yamashita, N. Sakai, T. Maruyama, E. Okuda, K. Hirano, S. Kihara, H. Hiraoka, and Y. Matsuzawa. 2000. Identification of a GPI-anchored type HDL-binding protein on human macrophages. *Biochem. Biophys. Res. Commun.* **272:** 864–871.
12. Boyum, A. 1968. Isolation of mononuclear cells and granulocytes from human blood. Isolation of mononuclear cells by one centrifugation, and of granulocytes by combining centrifugation and sedimentation at 1 g. *Scand. J. Clin. Lab. Invest.* **97 (Suppl.):** 77–89.
13. Havel, R. J., H. Eder, and J. H. Bradgon. 1955. The distribution and chemical composition of ultracentrifugally separated lipoproteins in human serum. *J. Clin. Invest.* **3:** 1345–1353.
14. Lowry, O. H., N. J. Rosenbrough, A. L. Farr, and R. J. Randall. 1951. Protein measurement with folin phenol reagent. *J. Biol. Chem.* **193:** 265–275.
15. Takata, K., S. Horiuchi, A. T. Rahim, and Y. Morino. 1988. Receptor-mediated internalization of high density lipoprotein by rat sinusoidal liver cells: identification of a nonlysosomal endocytic pathway by fluorescence-labeled ligand. *J. Lipid Res.* **29:** 1117–1126.
16. de la Llera Moya, M., V. Atger, J. L. Paul, N. Fournier, N. Moatti, P. Giral, K. E. Friday, and G. Rothblat. 1994. A cell culture system for screening human serum for ability to promote cellular cholesterol efflux. Relations between serum components and efflux, esterification, and transfer. *Arterioscler. Thromb. Vasc. Biol.* **14:** 1056–1065.
17. Sato, N., N. Funayama, A. Nagafuchi, S. Yonemura, S. Tsukita, and S. Tsukita. 1992. A gene family consisting of ezrin, radixin, and moesin: its specific localization at actin filament/plasma membrane association sites. *J. Cell Sci.* **103:** 131–143.
18. Sagara, J., S. Tsukita, S. Yonemura, S. Tsukita, and A. Kawai. 1995. Cellular actin-binding ezrin-radixin-moesin (ERM) family proteins are incorporated into the rabies virion and closely associated with viral envelope proteins in the cell. *Virology.* **206:** 485–494.
19. Mangeat, P., C. Roy, and M. Martin. 1999. ERM proteins in cell adhesion and membrane dynamics. *Trends Cell Biol.* **9:** 187–192.
20. Nakamura, F., L. Huang, K. Pestonjamasp, E. J. Luna, and H. Furthmayr. 1999. Regulation of F-actin binding to platelet moesin in vitro by both phosphorylation of threonine 558 and phosphosphatidylinositides. *Mol. Biol. Cell.* **10:** 2669–2685.
21. Tohme, Z. N., S. Amar, and T. E. van Dyke. 1999. Moesin functions as a lipopolysaccharide receptor on human monocytes. *Infect. Immun.* **67:** 3215–3220.
22. Ariel, A., R. Hershkoviz, I. Altbaum-Weiss, S. Ganor, and O. Lider. 2001. Cell surface-expressed moesin-like receptor regulates T cell interactions with tissue components and binds an adhesion-modulating IL-2 peptide generated by elastase. *J. Immunol.* **166:** 3052–3060.
23. Hecker, C., C. Weise, J. Schneider-Schaulies, H. C. Holmes, and V. ter Meulen. 1997. Specific binding of HIV-1 envelope protein gp120 to the structural membrane proteins ezrin and moesin. *Virus Res.* **49:** 215–223.

Increased lipid rafts and accelerated lipopolysaccharide-induced tumor necrosis factor-α secretion in Abca1-deficient macrophages[S]

Masahiro Koseki,[1,*] Ken-ichi Hirano,[*,†] Daisaku Masuda,[*] Chiaki Ikegami,[*] Masaki Tanaka,[§] Akemi Ota,[*] Jose C. Sandoval,[†] Yumiko Nakagawa-Toyama,[*] Satoshi B. Sato,[**] Toshihide Kobayashi,[††] Yukiko Shimada,[§§] Yoshiko Ohno-Iwashita,[§§] Fumihiko Matsuura,[*,†] Iichiro Shimomura,[*] and Shizuya Yamashita[*,†]

Department of Metabolic Medicine,[*] Cardiovascular Medicine,[†] and Medicine and Pathology,[§] Graduate School of Medicine, Osaka University, Suita, Osaka, Japan; Department of Biophysics,[**] Graduate School of Science, Kyoto University, Kyoto, Japan; RIKEN,[††] Wako, Saitama, Japan; and Biomembrane Research Group,[§§] Tokyo Metropolitan Institute of Gerontology, Itabashi-ku, Tokyo, Japan

Abstract **Lipid rafts on the cell surface are believed to be very important as platforms for various cellular functions. The aim of this study was to know whether defective lipid efflux may influence lipid rafts on the cell surface and their related cellular functions. We investigated macrophages with defective lipid efflux from ATP binding cassette transporter A1-deficient (Abca1-KO) mice. Lipid rafts were evaluated by the following two novel probes: a biotinylated and protease (subtilisin Carlsberg)-nicked derivative of θ-toxin and a fluorescein ester of polyethylene glycol-derived cholesterol. Lipid rafts in Abca1-KO macrophages were increased, as demonstrated by both probes. Moreover, activities of nuclear factor κB, mRNA and intracellular distribution, and secretion of tumor necrosis factor-α (TNF-α) were examined after stimulation by lipopolysaccharides (LPSs). LPS-induced responses of the activation of nuclear factor κB and TNF-α were more prompt and accelerated in the Abca1-KO macrophages compared with wild-type macrophages. Modification of lipid rafts by cyclodextrin and nystatin corrected the abnormal response, suggesting an association between the increased lipid rafts and abnormal TNF-α secretion. We report here that Abca1-KO macrophages with defective lipid efflux exhibited increased lipid rafts on the cell surface and accelerated TNF-α secretion.**—Koseki, M., K-i. Hirano, D. Masuda, C. Ikegami, M. Tanaka, A. Ota, J. C. Sandoval, Y. Nakagawa-Toyama, S. B. Sato, T. Kobayashi, Y. Shimada, Y. Ohno-Iwashita, F. Matsuura, I. Shimomura, and S. Yamashita. **Increased lipid rafts and accelerated lipopolysaccharide-induced tumor necrosis factor-α secretion in Abca1-deficient macrophages.** ***J. Lipid Res.*** **2007.** 48: **299–306.**

Supplementary key words ATP binding cassette transporter A1 • biotinylated and protease (subtilisin Carlsberg)-nicked derivative of θ-toxin • cholesterol efflux • lipid rafts • polyethylene glycol-derived cholesterol • tumor necrosis factor-α

Manuscript received 27 September 2006 and in revised form 31 October 2006.

Published, JLR Papers in Press, November 7, 2006.
DOI 10.1194/jlr.M600428-JLR200

Reverse cholesterol transport (RCT) is one of the major protective systems against atherosclerosis, in which HDL particles play a crucial role as a shuttle carrying cholesterol derived from peripheral tissues to the liver (1). Cholesterol efflux from the cells is the initial step of RCT, in which free apolipoprotein A-I (apoA-I) or small HDLs take up cholesterol from the peripheral cells. We have been trying to elucidate the molecular mechanism for RCT and cholesterol efflux by analyzing the pathophysiology of patients with abnormal HDL metabolism. We have identified molecules involved in cellular cholesterol efflux and apoA-I and HDL binding proteins on macrophages (2–5).

Tangier disease (TD) is a model for the impairment of cholesterol efflux from the cells (6, 7). Patients with TD suffer from genetic HDL deficiency, hepatosplenomegaly, orange tonsils, and premature atherosclerosis (8, 9). Many laboratories including ours have reported that mutations in the Abca1 gene lead to defective cholesterol efflux from the cells (10–12). As a result of the mutation(s) in the Abca1 gene, cells from TD patients exhibited a deficiency of apoA-I-mediated cholesterol efflux and a subsequent accumulation of intracellular lipids as lipid droplets, which is closely related to the development of atherosclerosis in this disorder.

On the other hand, in the plasma membrane, cholesterol is distributed abundantly in some domain structures

Abbreviations: Abca1-KO, ATP binding cassette transporter A1-deficient; apoA-I, apolipoprotein A-I; BCθ, biotinylated and protease (subtilisin Carlsberg)-nicked derivative of θ-toxin; fPEG-chol, fluorescent polyethylene glycol cholesteryl ether; LPS, lipopolysaccharide; NF-κB, nuclear factor-κB; 2OHpβCD, 2-hydroxypropyl-β-cyclodextrin; RCT, reverse cholesterol transport; TD, Tangier disease; TNF-α, tumor necrosis factor-α; WT, wild-type.

[1] To whom correspondence should be addressed.
e-mail: koseki@imed2.med.osaka-u.ac.jp

[S] The online version of this article (available at http://www.jlr.org) contains supplementary data in the form of figures.

called "lipid rafts," "cholesterol-rich microdomains," or "detergent-resistant membranes" (13). These domains are enriched in cholesterol and sphingolipids and contain specific proteins, including glycosylphosphatidylinositol-anchored proteins, and are believed to be important as rafts mediating some intracellular and/or extracellular signals (14–20). Recently, the following two probes were developed to visualize rafts. One is a biotinylated and protease (subtilisin Carlsberg)-nicked derivative of θ-toxin (BCθ) (21–25). This probe was developed by Ohno-Iwashita et al. (21–25) and is derived from a thiol-activated cytolysin produced by *Clostridium perfringens*. BCθ selectively binds to membrane cholesterol in lipid rafts. The other probe is a polyethylene glycol cholesteryl ether (26, 27). This compound belongs to a unique group of nonionic amphipathic cholesterol derivatives. It can bind with cholesterol-rich membranes both in cells and in model membranes. It was recently reported that a fluorescent polyethylene glycol cholesteryl ether (fPEG-chol) is a sensitive probe for unraveling the dynamics of cholesterol-rich microdomains in living cells.

Little is known about the effect of defective lipid efflux on lipid rafts in plasma membranes. In this study, we have tested the hypothesis that defective efflux influences lipid rafts in the plasma membrane and examined related cellular functions using ATP binding cassette transporter A1-deficient (Abca1-KO) macrophages as a model.

METHODS

Materials

BCθ and fPEG-chol were prepared as described previously (26, 28).

Animal treatment and cell culture

Abca1-KO mice created on the DBA1 lac/J background (29) were purchased from the Jackson Laboratory. Mice were fed a normal chow diet. The experimental protocol was approved by the Ethics Review Committee for Animal Experimentation of Osaka University Graduate School of Medicine. After an intraperitoneal injection of 2 ml of 4% thioglycollate (B-2551; Sigma-Aldrich) medium, mouse peritoneal macrophages were harvested from Abca1-KO and wild-type (WT) mice. The cells were cultured according to standard conditions in Dulbecco's minimum essential medium supplemented with L-glutamine, nonessential amino acids, and 10% fetal calf serum in a humidified 5% CO_2 atmosphere at 37°C. Human monocyte-derived macrophages from a TD patient and healthy volunteers were prepared after informed consent was obtained. ABCA1-null fibroblasts were obtained from two unrelated male patients with TD after informed consent was obtained.

Fluorescence labeling for confocal laser microscopy

The cells were washed with ice-cold PBS and treated with 10 μg/ml BCθ for 30 min on ice. After rinsing, the cells were fixed with 4% formaldehyde and incubated with streptavidin-Alexa Flour 594 conjugate for 30 min (S-11227; Molecular Probes). The nuclei were stained with 4′,6-diamino-phenylindole. In other experiments for fPEG-chol, cells were fixed and treated with 0.2% gelatin for 30 min and then incubated with 1 μg/ml fPEG-chol for 5 min at room temperature. Images were acquired for each fluorescent probe by confocal laser microscopy (LSM510; Carl Zeiss).

Fractionation by sucrose density gradient ultracentrifugation

After incubation with 10 μg/ml BCθ for 30 min on ice, mouse peritoneal macrophages were harvested and sucrose gradient ultracentrifugation was performed as described previously (25). Free cholesterol levels were measured using the Amplex Red cholesterol assay method (Molecular Probes) (25).

Detection of BCθ bound to cells by Western blot analysis

The lysates of BCθ-bound cells were subjected to SDS-PAGE, and Western blot analysis was performed as described previously (25).

Construction of adenovirus vectors and their expression in fibroblasts

FLAG-tagged human Abca1 cDNA with the FLAG epitope (DYKDDDDK) incorporated at its C terminus (hAbca1/FLAG) was generated by PCR. Adenovirus vectors encoding LacZ and hAbca1/FLAG were constructed according to the protocol of the Adeno X expression system (Clontech). Infection with adenovirus was carried out by incubating cells in serum-free medium for 1 h at 37 °C under gentle agitation. After incubation, complete medium was supplied, and the cells were further incubated in a CO_2 incubator. Five days after infection with the indicated multiplicity of infection, the cells were used in the experiments.

Measurement of tumor necrosis factor-α levels and nuclear factor-κB p65 activities

The mouse peritoneal macrophages were plated on 24-well plates and incubated with 10 ng/ml lipopolysaccharide (LPS) of *Escherichia coli* strain O55:B5 (L-6529; Sigma-Aldrich). The amount of tumor necrosis factor-α (TNF-α) in the culture medium was determined by ELISA (mouse TNF-α ELISA kit; Biosource). Nucleoproteins were extracted from the macrophages (Nuclear Extract Kit; Active Motif), and nuclear factor-κB (NF-κB) p65 activity was measured according to the manufacturer's protocols (TransAM NF-κB p65 Chemi; Active Motif).

RNA isolation, cDNA synthesis, and quantitative PCR

Total RNA was isolated from mouse macrophages using the RNeasy Mini Kit (Qiagen), followed by treatment with DNase I (Qiagen). Of each RNA sample, 1 μg of total RNA was primed with 50 pmol of oligo(dT)20 and reverse-transcribed with SuperScript III RT (200 units; Invitrogen), according to the protocol of the manufacturer. Real-time quantitative PCR was performed according to the protocol of the DyNAmo HS SYBR Green quantitative PCR kit. To assess the expression levels of TNF-α mRNA in macrophages, DNA polymerase and SYBR Green I were used in a reaction volume of 20 μl using gene-specific primers (5 mM) on cDNA (corresponding to ~50 ng of total RNA) (8, 30).

Primers used in this study

Each set of primers located different exons: primer 1, 5′-ccagaccctcacactcagatca-3′, mouse TNF-α cDNA, nucleotides 381–402 (GenBank accession number NM_013693); primer 2, 5′-cacttggtggtttgctacgac-3′, mouse TNF-α cDNA, nucleotides 459–439 (GenBank accession number NM_013693); primer 3, 5′-ggagccaaacggggtcatcatctc-3′, mouse GAPDH cDNA, nucleotides 383–405 (GenBank accession number M32599); primer

4, 5′-gaggggccatccacagtcttct-3′, mouse GAPDH cDNA, nucleotides 615–594 (GenBank accession number M32599).

RESULTS

Lipid rafts were increased in Abca1-KO macrophages

Lipid rafts on the plasma membrane were visualized using two different probes, BCθ and fPEG-chol. Confocal laser scanning microscopy revealed that both probes recognized a greater volume of lipid rafts in the mouse peritoneal macrophages from Abca1-KO mice than from WT mice (**Fig. 1A**). Similar results were obtained in human monocyte-derived macrophages from a TD patient (9) and from normal subjects (Fig. 1B). These results suggested that lipid rafts on the plasma membrane were increased in Abca1-KO macrophages. As the number of the patient macrophages was limited, we made use of mouse macrophages in the experiments described below.

To confirm whether BCθ recognizes cholesterol-rich domains in mouse peritoneal macrophages, sucrose density gradient ultracentrifugation was performed. In both Abca1-KO and WT macrophages, the distribution of free cholesterol concentration consisted of two peaks: low density raft fractions (fractions 2–5) and high density nonraft fractions (fractions 8–10) (**Fig. 2A**). The sums of cholesterol content in the raft fractions (fractions 2–5) and in the nonraft fractions (fractions 8–10) were calculated, showing that the free cholesterol content of lipid rafts was increased significantly in Abca1-KO macrophages and that the free cholesterol content of nonrafts was not significantly different between WT and Abca1-KO macrophages (Fig. 2B). As expected, BCθ was distributed mainly in low-density, Triton X-100-insoluble membrane fractions (fractions 2–5), as shown by Western blot analysis, in both Abca1-KO and WT macrophages, and BCθ binding to rafts of Abca1-KO macrophages was detected more strongly than to rafts of WT macrophages (Fig. 2A).

Abca1 complementation corrected abnormal lipid rafts

Furthermore, to analyze the relationship between Abca1 and lipid rafts, we performed a complementary experiment using TD fibroblasts. The lipid rafts in TD fibroblasts were increased (see supplementary Fig. IA). We generated the adenovirus encoding human Abca1 and examined its effect on binding of BCθ to TD fibroblasts. Confocal laser scanning microscopy and Western blot analysis clearly showed a multiplicity of infection-dependent decrease in BCθ binding (see supplementary Fig. IB). This result indicated that introduction of the Abca1 gene corrected the phenotype of TD fibroblasts, suggesting a causal relationship between Abca1 deficiency and the alteration of lipid rafts.

Abnormal cytokine secretion from Abca1-KO macrophages

We supposed that the increase of lipid rafts, as well as intracellular lipid storage, might affect the process of premature atherosclerosis in patients with TD. We hypothesized that the increase of lipid rafts might affect the activation of nuclear receptors and the subsequent synthesis and secretion of cytokines in macrophages, because some papers reported that lipid rafts might play a pivotal role in the cellular recognition of LPS (31). Therefore, we focused on LPS-induced intracellular signaling and cytokine secretion, particularly at an acute phase after

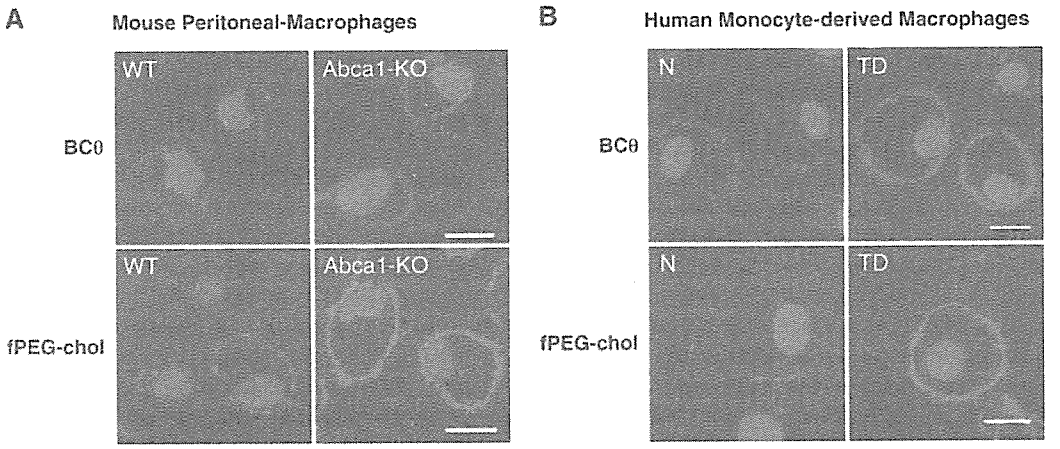

Fig. 1. Visualized lipid rafts in mouse and human macrophages. A: ATP binding cassette transporter A1-deficient (Abca1-KO) and wild-type (WT) mouse peritoneal macrophages were washed once with ice-cold PBS and treated with 10 μg/ml biotinylated and protease (subtilisin Carlsberg)-nicked derivative of θ-toxin (BCθ) for 30 min on ice. After rinsing, the cells were fixed with 4% formaldehyde and incubated with streptavidin-Alexa Flour 594 conjugate (S-11227; Molecular Probes) for 30 min (red). The nuclei were stained with 4′,6-diamino-phenylindole (blue). In the experiments for fluorescent polyethylene glycol cholesteryl ether (fPEG-chol), macrophages were fixed and treated with 0.2% gelatin for 30 min, then incubated with 0.5 μg/ml fPEG-chol for 5 min (green). Images were acquired for each fluorescent probe by confocal laser microscopy (LSM510; Carl Zeiss). The results shown are representative of three independent experiments. Bars = 10 μm. B: Human monocyte-derived macrophages from a Tangier disease (TD) patient and a normal subject (N) were also examined. The results shown are a representative of three independent experiments. Bars = 10 μm.

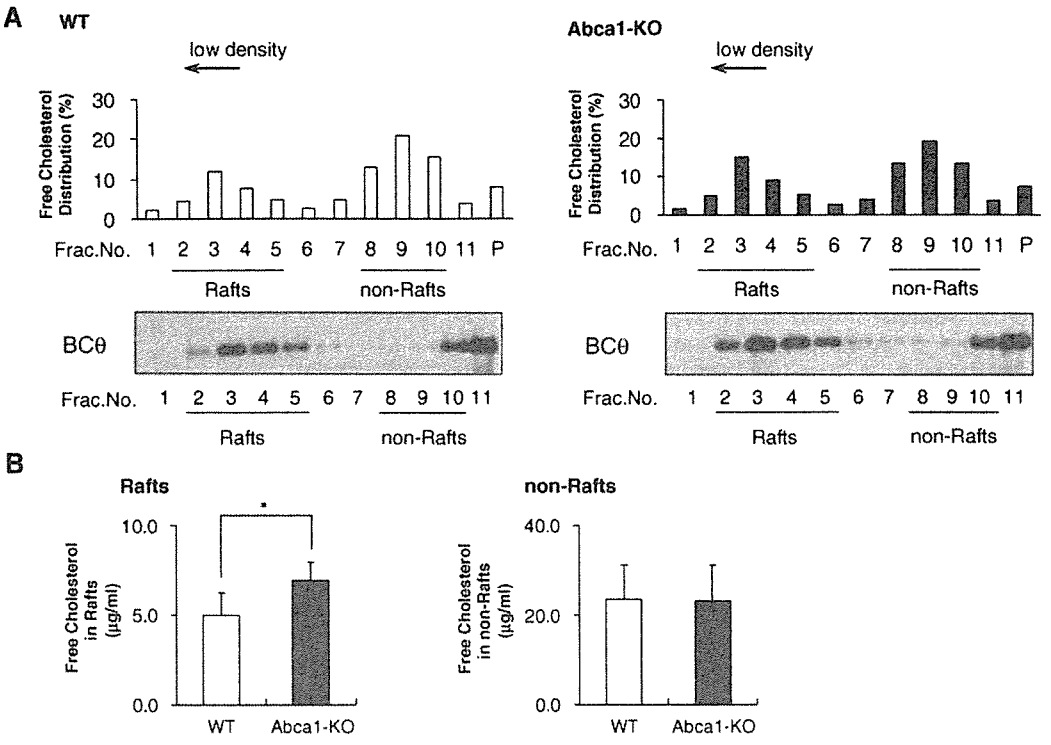

Fig. 2. Sucrose gradient fractionation confirmed that BCθ recognized lipid rafts in mouse peritoneal macrophages. A: BCθ-treated mouse macrophages were incubated with 1% Triton X-100 at 4°C for 30 min. Equal amounts of protein homogenates were subjected to sucrose gradient ultracentrifugation and fractionated from the top [fractions 1–11 and pellet (P); the pellet was suspended and sonicated in buffered saline], as described in Methods. To determine the distribution of free cholesterol and BCθ, the same volume of each fraction was subjected to the quantification of cholesterol and Western blot analysis. BCθ binding to lipid rafts in Abca1-KO and WT macrophages was selectively detected in Triton X-100-insoluble raft fractions by Western blot analysis. The amount of BCθ binding to lipid rafts in Abca1-KO macrophages was greater than that in WT macrophages. The signals of BCθ in the bottom fraction 11 seemed to be free BCθ. The results shown are representative of three independent experiments. B: The sums of cholesterol contents in lipid raft fractions (fractions 2–5) and in nonlipid raft fractions (fractions 8–10) were compared between Abca1-KO and WT macrophages. Free cholesterol contents were significantly higher in lipid rafts of Abca1-KO macrophages than in those of WT macrophages. Values shown are mean ± SEM. * $P < 0.05$ by Student's *t*-test.

LPS stimulation. As shown in **Fig. 3A**, activities of NF-κB p65 were induced only at 15 min in both Abca1-KO and WT macrophages, and the activity was significantly higher in Abca1-KO macrophages than in WT macrophages throughout the time course. Figure 3B shows the TNF-α mRNA levels. TNF-α mRNA levels were induced at 30 min and reached a peak at 45 min in both Abca1-KO and WT macrophages. TNF-α mRNA in Abca1-KO macrophages was significantly higher than in WT macrophages at any time point after 30 min. Figure 3C demonstrates the immunocytochemical analysis for TNF-α (32). Before LPS stimulation, we could not detect the immunoreactive mass of TNF-α in either macrophages. After 1 h, the immunoreactive mass of TNF-α was detected in perinuclear organelles in Abca1-KO macrophages but not in WT macrophages. After 2 h, the immunoreactive mass of TNF-α was found more dispersed in the cytoplasm of Abca1-KO macrophages. Figure 3D shows TNF-α secretion data. A significant difference in TNF-α secretion into the medium occurred at 1 h after LPS stimulation. Similarly, the secretion of interleukin-6 into the medium was significantly higher in Abca1-KO macrophages than in WT macrophages (see supplementary Fig. II). These data suggest that an acute phase response to LPS seems to be accelerated in Abca1-KO macrophages.

Effect of lipid raft modulators on mRNA and release of TNF-α

Finally, we investigated the relationship between increased lipid rafts and the accelerated response of TNF-α in Abca1-KO macrophages. We used the following two lipid raft modulators: 2-hydroxypropyl-β-cyclodextrin (2OHpβCD) and nystatin (21, 31, 33). **Figure 4A** shows the effect of 2OHpβCD, which selectively depleted cholesterol from lipid rafts, on staining with BCθ. The signals of BCθ were diminished after 2OHpβCD treatment in both macrophages. Figure 4B indicates the effect of the depletion of rafts on TNF-α mRNA levels and TNF-α secretion from macrophages. After treatment with 20 mM 2OHpβCD, the LPS-induced expression of TNF-α was decreased significantly in Abca1-KO and WT macrophages. The depletion of cholesterol from rafts by treatment with 20 mM 2OHpβCD diminished the significant difference in TNF-α mRNA levels and TNF-α secretion between Abca1-

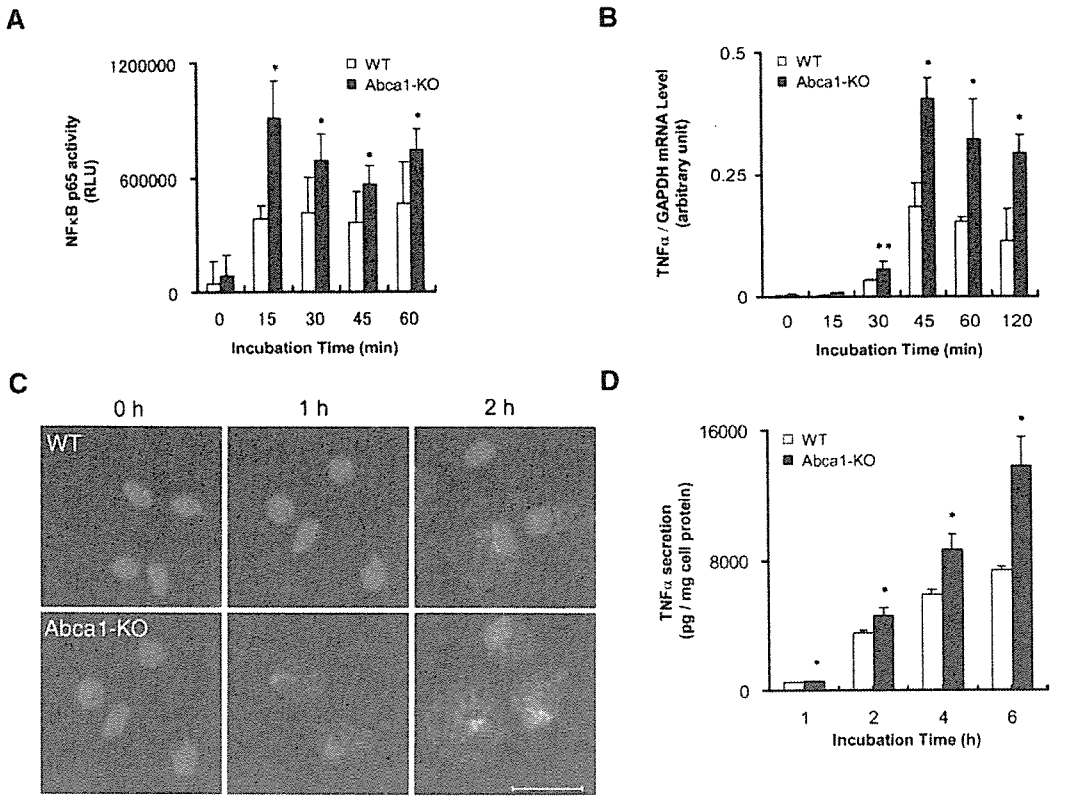

Fig. 3. Activities of nuclear factor-κB (NF-κB) and mRNA and release of tumor necrosis factor-α (TNF-α) from Abca1-KO macrophages. The 1.5×10^6 peritoneal macrophages of Abca1-KO or WT mice were seeded on 24-well plates. After 2 days, the macrophages were incubated with 10 ng/ml lipopolysaccharide (LPS) of *Escherichia coli* strain O55:B5 (L-6529; Sigma-Aldrich) for the indicated time in each experiment. A: Nucleoprotein was extracted from the macrophages (Nuclear Extract Kit; Active Motif), and NF-κB p65 activity was measured (TransAM NF-κB p65 Chemi; Active Motif). B: Total RNA was isolated from the macrophages, and TNF-α mRNA levels were evaluated by real-time quantitative PCR. C: The macrophages were fixed and stained with goat anti-TNF-α antibody (Molecular Probes) and goat anti-Alexa Flour 488. The nuclei were stained with 4′,6-diamino-phenylindole. Images were acquired by confocal laser microscopy (LSM510; Carl Zeiss). Bar = 20 μm. D: TNF-α in the medium was measured by ELISA (mouse TNF-α ELISA kit; Biosource). Means and SD values were calculated from the data from three independent experiments. * $P < 0.05$, ** $P < 0.01$ by Student's *t*-test.

KO and WT macrophages. Next, as shown in Fig. 4C, we tested another lipid raft modulator, nystatin, which was shown to disrupt cholesterol-rich domains. After treatment with nystatin, the expression of TNF-α was also decreased significantly in both macrophages. Treatment with 25 μg/ml nystatin attenuated the significant difference of TNF-α mRNA levels between Abca1-KO and WT macrophages. These data strongly suggested that Abca1-KO macrophages were more affected by lipid raft modulators because of the increase of lipid rafts. The alteration of lipid rafts may regulate the acute response of TNF-α by LPS stimulation.

DISCUSSION

Lipid rafts and atherosclerosis

Lipid bilayers in the plasma membrane were previously believed to be homogeneous. Recently, a number of studies revealed that lipid rafts could play an essential role in many cellular processes, including signal transduction, membrane trafficking, cytoskeletal organization, and many other cellular events (17–20, 34, 35). Even though many studies focused on the distribution pattern of membrane proteins in lipid rafts, there is little evidence that a particular genetic defect might affect the number of lipid rafts and subsequent cellular functions. One reason for this might be the complexity and difficulty of measuring lipid rafts. In this study, we have succeeded relatively easily in comparing the volume of lipid rafts using two newly developed lipid raft probes. Here, for the first time, we report that a mutation in a single gene might alter lipid rafts and that the increase in lipid rafts might be related to the acceleration of atherogenic processes. In this study, we focused on the acute secretion to LPS stimulation. Recently, Ishiwata et al. (26) and Kay et al. (36) reported on the importance of cholesterol-rich lipid rafts in the delivery of TNF-α to the plasma membrane and the exit sites for cytokine secretion. It would be of interest to investigate whether the increased lipid rafts in the Abca1-KO macrophages might affect the exocytosis of cytokines. Further studies will be necessary to clarify this.

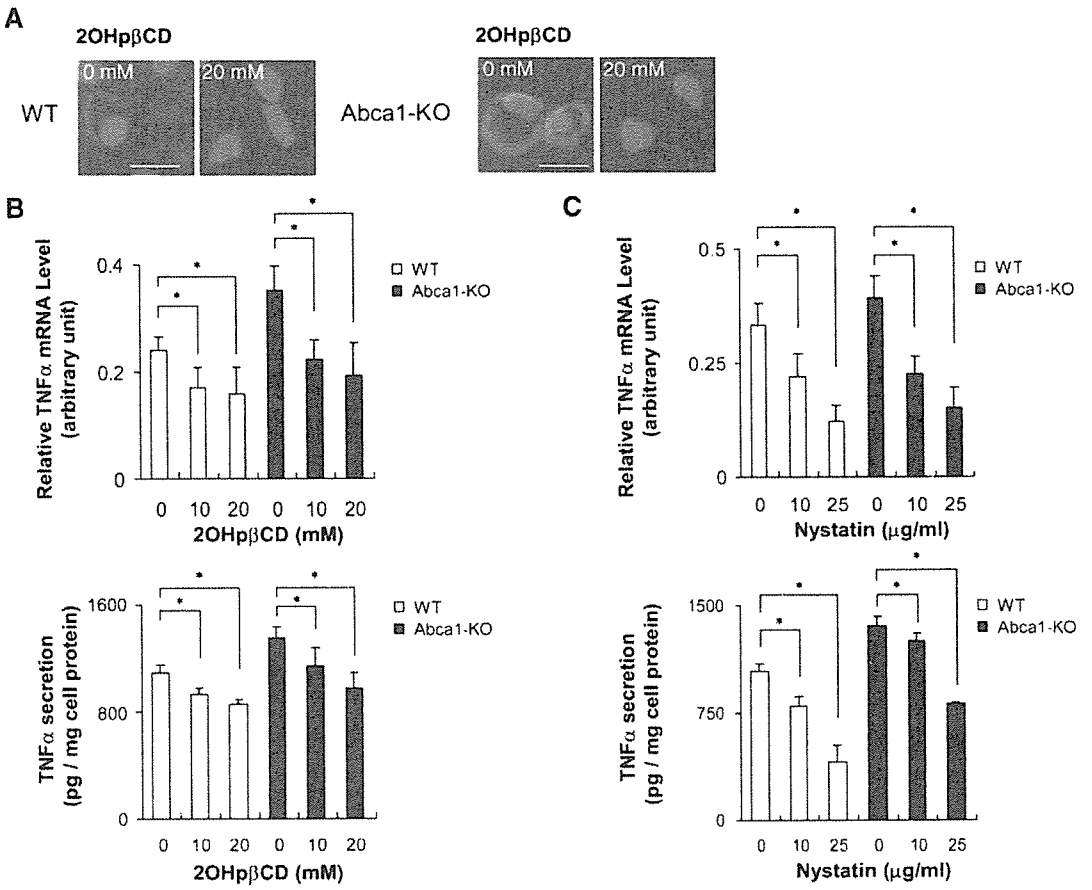

Fig. 4. Effect of lipid raft modulators on mRNA and secretion of TNF-α. A: To deplete cholesterol from lipid rafts, the macrophages were treated with 2-hydroxypropyl-β-cyclodextrin (2OHpβCD) (18847-64; Nacalai Tesque) for 30 min on ice. After treatment, the Abca1-KO and WT macrophages were stained with 10 μg/ml BCθ and streptavidin-Alexa Flour 594 conjugate, as described in Methods (red). The nuclei were stained with 4′,6-diamino-phenylindole (blue). Images were acquired by confocal laser microscopy. Bars = 10 μm. B: After treatment with 2OHpβCD for 30 min, the Abca1-KO and WT macrophages were stimulated by 10 ng/ml LPS at 37°C. TNF-α mRNA levels after 30 min and TNF-α secretion into the medium during 1 h were quantified, as described in Methods. C: To disrupt cholesterol-rich domains, the Abca1-KO and WT macrophages were treated with nystatin (N-6261; Sigma-Aldrich) for 5 min on ice. After treatment with nystatin, the macrophages were stimulated by 10 ng/ml LPS at 37°C. TNF-α mRNA levels after 30 min and TNF-α secretion into the medium during 1 h were measured. Mean and SD values were calculated from the data from three independent experiments. * $P < 0.05$ by Student's *t*-test.

Abca1 deficiency may accelerate atherosclerosis mediated by the increase of lipid rafts

TD is a familial HDL deficiency, which is a model for impaired cholesterol efflux, the initial step of RCT, and is frequently associated with cardiovascular diseases. We previously reported that a patient with TD suffered from severe coronary atherosclerosis using intravascular ultrasonography (9). Many previous studies have indicated that TD is associated with mutations in the Abca1 gene and that the loss of function of Abca1 led to defective cholesterol and phospholipid efflux from macrophages, followed by intracellular lipid accumulation, foam cell formation, and atherosclerosis (**Fig. 5**, left). In this study, we have shown another aspect of TD: that impaired cholesterol efflux may cause the deposition of free cholesterol in lipid rafts (Fig. 5, right) and that the increased lipid rafts may play a principal role in the regulation of the acute response of TNF-α to LPS stimulation. These observations may indicate that premature atherosclerosis in patients with TD may be accelerated by enhanced inflammation through an abnormality of lipid rafts. In vivo, the increased TNF-α levels in the plasma of Abca1-KO mice or TD patients have not been reported. Further studies will be necessary to clarify this issue.

During the preparation of our manuscript, Landry et al. (37) reported the unique relationship between Abca1 expression and membrane microdomains. They used BHK cells expressing a functional Abca1 or a nonfunctional Abca1 with a mutation in the ATP binding domain. They clearly showed that the overexpression of Abca1 results in the disruption of microdomains through its ATPase-related functions. On the other hand, we focused on the cause of TD and independently investigated the macrophages derived from a patient with TD and Abca1-KO mice. We demonstrated the increase in lipid rafts with two newly developed probes recognizing cholesterol directly

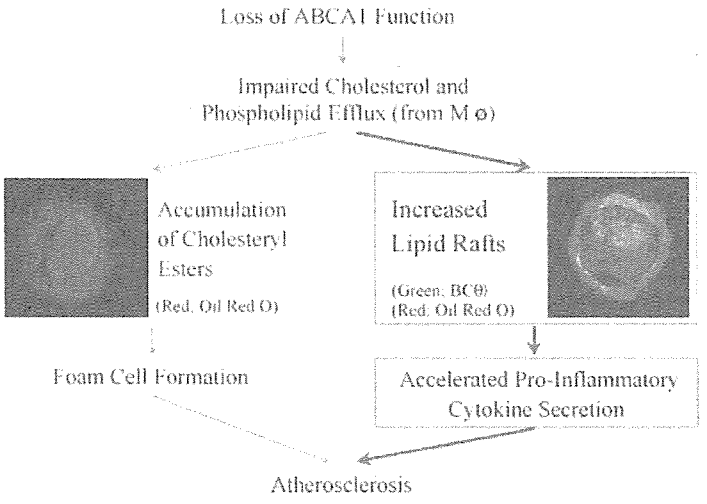

Fig. 5. A novel phenotype may accelerate atherosclerosis in Abca1-KO macrophages. Many studies have indicated that the loss of function of Abca1 causes the defective cholesterol and phospholipid efflux from macrophages, followed by the accumulation of cholesteryl esters, foam cell formation, and atherosclerosis. In this study, we revealed another novel phenotype of Abca1 deficiency: that impaired cholesterol efflux may influence plasma membrane lipid composition. Increased lipid rafts represent an important platform for the LPS-induced response and an accelerated proinflammatory cytokine release. Double staining with Oil Red O (red) and BCθ (green) made it possible to show cell surface free cholesterol and intracellular cholesteryl esters (lipid droplets) simultaneously and distinctly. Both panels show human monocyte-derived macrophages from a patient with TD.

and suggested accelerated TNF-α secretion under Abca1-KO conditions. Together, these data strongly demonstrate that Abca1 might be involved in the regulation and formation of lipid rafts in plasma membranes.

Cholesterol deposition and inflammation in macrophages

It is widely believed that inflammation might contribute to the progression of atherosclerosis. However, the relationship between intracellular lipid storage and inflammation in macrophages has not been clarified. Some studies revealed the relationship between cholesterol deposition and cytokine secretion in macrophages. Li et al. (38) demonstrated that TNF-α and interleukin-6 were induced in free cholesterol-loaded macrophages without LPS stimulation. They speculated that an excess storage of endoplasmic reticulum cholesterol may be the cause. Our data raised the possibility that cholesterol deposition in plasma membranes might affect the accelerated induction of TNF-α. On the other hand, Francone et al. (39) reported an observational study about the intracellular lipid storage and proinflammatory conditions of Abca1 and LDL receptor double knockout macrophages. In our study, we revealed one of the molecular mechanisms for this, showing that the increased lipid rafts may result in abnormal cytokine release.

Lipid rafts as a therapeutic target

Abca1 plays a key role in the regulation of cholesterol homeostasis and the function of macrophages. We demonstrated the relationship between Abca1 and lipid rafts using Abca1-defective animal and human models. On the other hand, in Abca1-expressing macrophages, the function of Abca1 was altered under some conditions. Wang and Oram (40, 41) reported that unsaturated fatty acids reduced Abca1 expression in macrophages by enhancing its degradation rate. These findings might support the speculation that the Abca1 of normal macrophages might be destabilized by unsaturated fatty acids, resulting in alterations of lipid rafts. The alteration of lipid rafts should be investigated in other atherogenic conditions affecting lipid efflux. In this study, we demonstrated that an extremely short-time modification of lipid composition in plasma membranes, using lipid raft modulators, might be a novel therapeutic strategy to attenuate acute accelerated proinflammatory events in macrophages.

Conclusion

Abca1-KO macrophages with defective lipid efflux exhibited increased lipid rafts on the cell surface and accelerated TNF-α release, which is a novel phenotype of macrophages with defective lipid efflux. Thus, modulation of Abca1 and lipid rafts may become a novel therapeutic target to prevent atherosclerosis.

This work was supported by Grants-in-Aid 11557055 and 10671070 to S.Y. and 13671191 to K-i.H. from the Ministry of Education, Science, Sports, and Culture of Japan. This work was also supported by a grant from the Japan Society for the Promotion of Science to S.Y. and Z. Zhang. This research was partially supported by an International HDL Research Awards Program grant from Pfizer, a grant from the Novartis Foundation for Gerontological Research, a grant from the Takeda Medical Research Foundation, and a grant from the Ono Medical Foundation to S.Y.

REFERENCES

1. Glomset, J. A. 1968. The plasma lecithin:cholesterol acyltransferase reaction. *J. Lipid Res.* **9:** 155–167.
2. Hirano, K., F. Matsuura, K. Tsukamoto, Z. Zhang, A. Matsuyama, K. Takaishi, R. Komuro, T. Suehiro, S. Yamashita, Y. Takai, et al. 2000. Decreased expression of a member of the Rho GTPase family, Cdc42Hs, in cells from Tangier disease—the small G protein may play a role in cholesterol efflux. *FEBS Lett.* **484:** 275–279.
3. Zhang, Z., K. Hirano, K. Tsukamoto, C. Ikegami, M. Koseki, K. Saijo, T. Ohno, N. Sakai, H. Hiraoka, I. Shimomura, et al. 2005. Defective cholesterol efflux in Werner syndrome fibroblasts and its phenotypic correction by Cdc42, a RhoGTPase. *Exp. Gerontol.* **40:** 286–294.
4. Tsukamoto, K., K. Hirano, K. Tsujii, C. Ikegami, Z. Zhang, Y. Nishida, T. Ohama, F. Matsuura, S. Yamashita, and Y. Matsuzawa. 2001. ATP-binding cassette transporter-1 (ABCA1) induces rear-

rangement of actin cytoskeletons possibly through Cdc42/N-WASP. *Biochem. Biophys. Res. Commun.* **287:** 757–765.
5. Hirano, K., S. Yamashita, Y. Nakagawa, T. Ohya, F. Matsuura, K. Tsukamoto, Y. Okamoto, A. Matsuyama, K. Matsumoto, J. Miyagawa, et al. 1999. Expression of human scavenger receptor class B type I in cultured human monocyte-derived macrophages and atherosclerotic lesions. *Circ. Res.* **85:** 108–116.
6. Assmann, G., A. Eckardstein, and H. B. Brewer. 2001. Familial analphalipoproteinemia: Tangier disease. *In* Metabolic and Molecular Bases of Inherited Diseases. 8th edition. Vol. 2. McGraw Hill, New York. 2937–2960.
7. Oram, J. F., and S. Yokoyama. 1996. Apolipoprotein-mediated removal of cellular cholesterol and phospholipids. *J. Lipid Res.* **37:** 1503–1521.
8. Nishida, Y., K. Hirano, K. Tsukamoto, M. Nagano, C. Ikegami, K. Roomp, M. Ishihara, N. Sakane, Z. Zhang, K. Tsujii, et al. 2002. Expression and functional analyses of novel mutations of ATP-binding cassette transporter-1 in Japanese patients with high-density lipoprotein deficiency. *Biochem. Biophys. Res. Commun.* **290:** 713–721.
9. Komuro, R., S. Yamashita, S. Sumitsuji, K. Hirano, T. Maruyama, M. Nishida, F. Matsuura, A. Matsuyama, T. Sugimoto, N. Ouchi, et al. 2001. Tangier disease with continuous massive and longitudinal diffuse calcification in the coronary arteries: demonstration by the sagittal images of intravascular ultrasonography. *Circulation.* **101:** 2446–2448.
10. Brooks-Wilson, A., M. Marcil, S. M. Clee, L. H. Zhang, K. Roomp, M. V. Dam, L. Yu, C. Brewer, J. A. Collins, H. O. Molhuizen, et al. 1999. Mutations in ABC1 in Tangier disease and familial high-density lipoprotein deficiency. *Nat. Genet.* **22:** 336–345.
11. Bodzioch, M., E. Orso, J. Klucken, T. Langmann, A. Bottcher, W. Diederich, W. Drobnik, S. Barlage, C. Buchler, M. Porsch-Ozcurumez, et al. 1999. The gene encoding ATP-binding cassette transporter 1 is mutated in Tangier disease. *Nat. Genet.* **22:** 347–351.
12. Rust, S., M. Rosier, H. Funke, J. Real, Z. Amoura, J. C. Piette, J. F. Deleuze, H. B. Brewer, N. Duverger, P. Denefle, et al. 1999. Tangier disease is caused by mutations in the gene encoding ATP-binding cassette transporter 1. *Nat. Genet.* **22:** 352–355.
13. Pike, L. J. 2006. Rafts defined: a report on the Keystone symposium on lipid rafts and cell function. *J. Lipid Res.* **47:** 1597–1598.
14. Simons, K., and E. Ikonen. 1997. Functional rafts in cell membranes. *Nature.* **387:** 569–572.
15. Anderson, R. G., and K. Jacobson. 2002. A role for lipid shells in targeting proteins to caveolae, rafts, and other lipid domains. *Science.* **296:** 1821–1825.
16. Drobnik, W., H. Borsukova, A. Bottcher, A. Pfeiffer, G. Liebisch, G. J. Schutz, H. Schindler, and G. Schmitz. 2002. Apo AI/ABCA1-dependent and HDL3-mediated lipid efflux from compositionally distinct cholesterol-based microdomains. *Traffic.* **3:** 268–278.
17. Macdonald, J. L., and L. J. Pike. 2005. A simplified method for the preparation of detergent-free lipid rafts. *J. Lipid Res.* **46:** 1061–1067.
18. Gaus, K., M. Rodriguez, K. R. Ruberu, I. Gelissen, T. M. Sloane, L. Kritharides, and W. Jessup. 2005. Domain-specific lipid distribution in macrophage plasma membranes. *J. Lipid Res.* **46:** 1526–1538.
19. Li, Q., M. Wang, L. Tan, C. Wang, J. Ma, N. Li, Y. Li, G. Xu, and J. Li. 2005. Docosahexaenoic acid changes lipid composition and interleukin-2 receptor signaling in membrane rafts. *J. Lipid Res.* **46:** 1904–1913.
20. Urano, Y., I. Hayashi, N. Isoo, P. C. Reid, Y. Shibasaki, N. Noguchi, T. Tomita, T. Iwatsubo, T. Hamakubo, and T. Kodama. 2005. Association of active gamma-secretase complex with lipid rafts. *J. Lipid Res.* **46:** 904–912.
21. Waheed, A. A., Y. Shimada, H. F. G. Heijen, M. Nakamura, M. Inomata, M. Hayashi, S. Iwashita, J. W. Slot, and Y. Ohno-Iwashita. 2001. Selective binding of perfringolysin O derivative to cholesterol-rich membrane microdomains (rafts). *Proc. Natl. Acad. Sci. USA.* **98:** 4926–4931.
22. Ohno-Iwashita, Y., Y. Shimada, A. A. Waheed, M. Hayashi, M. Inomata, M. Nakamura, M. Maruya, and S. Iwashita. 2004. Perfringolysin O, a cholesterol-binding cytolysin, as a probe for lipid rafts. *Anaerobe.* **10:** 125–134.
23. Reid, P. C., N. Sakashita, S. Sugii, Y. Ohno-Iwashita, Y. Shimada, W. F. Hickey, and T. Y. Chang. 2004. A novel cholesterol stain reveals early neuronal cholesterol accumulation in the Niemann-Pick type C1 mouse brain. *J. Lipid Res.* **45:** 582–591.
24. Ohno-Iwashita, Y., M. Iwamoto, S. Ando, and S. Iwashita. 1992. Effect of lipidic factors on membrane cholesterol topology: mode of binding of θ-toxin to cholesterol on liposomes. *Biochim. Biophys. Acta.* **1109:** 81–90.
25. Nakamura, M., H. Kondo, Y. Shimada, A. A. Waheed, and Y. Ohno-Iwashita. 2003. Cellular aging-dependent decrease in cholesterol in membrane microdomains of human diploid fibroblasts. *Exp. Cell Res.* **290:** 381–390.
26. Ishiwata, H., S. B. Sato, A. Vertut-Doi, Y. Hamashima, and K. Miyajima. 1997. Cholesterol derivative of poly (ethylene glycol) inhibits clathrin-independent, but not clathrin-dependent endocytosis. *Biochim. Biophys. Acta.* **1359:** 123–135.
27. Sato, S. B., K. Ishii, A. Makino, K. Iwabuchi, A. Yamaji-Hasegawa, Y. Senoh, I. Nagaoka, H. Sakuraba, and T. Kobayashi. 2004. Distribution and transport of cholesterol-rich membrane domains monitored by a membrane-impermeant fluorescent polyethylene glycol-derivatized cholesterol. *J. Biol. Chem.* **279:** 23790–23796.
28. Iwamoto, M., I. Morita, M. Fukuda, S. Murota, S. Ando, and Y. Ohno-Iwashita. 1997. A biotinylated perfringolysin O derivative: a new probe for detection of cell surface cholesterol. *Biochim. Biophys. Acta.* **1327:** 222–230.
29. McNeish, J., R. J. Aiello, D. Guyot, T. Turi, C. Gabel, C. Aldinger, K. L. Hoppe, M. L. Roach, L. J. Royer, J. Wet, et al. 2000. High density lipoprotein deficiency and foam cell accumulation in mice with targeted disruption of ATP-binding cassette transporter-1. *Proc. Natl. Acad. Sci. USA.* **97:** 4245–4250.
30. Ohama, T., K. Hirano, Z. Zhang, R. Aoki, K. Tsujii, Y. Nakagawa-Toyama, K. Tsukamoto, C. Ikegami, A. Matsuyama, M. Ishigami, et al. 2002. Dominant expression of ATP-binding cassette transporter-1 on basolateral surface of Caco-2 cells stimulated by LXR/RXR ligands. *Biochem. Biophys. Res. Commun.* **296:** 625–630.
31. Triantafilou, M., K. Miyake, D. T. Golenbock, and K. Triantafilou. 2002. Mediators of innate immune recognition of bacteria concentrate in lipid rafts and facilitate lipopolysaccharide-induced cell activation. *J. Cell Sci.* **115:** 2603–2611.
32. Murray, R. Z., F. G. Wylie, T. Khromykh, D. A. Hume, and J. L. Stow. 2005. Syntaxin 6 and Vti1b form a novel SNARE complex, which is up-regulated in activated macrophages to facilitate exocytosis of tumor necrosis factor-alpha. *J. Biol. Chem.* **280:** 10478–10483.
33. Brown, D. A., and J. K. Rose. 1992. Sorting of GPI-anchored proteins to glycolipid-enriched membrane subdomains during transport to the apical cell surface. *Cell.* **68:** 533–544.
34. Munro, S. 2003. Lipid rafts: elusive or illusive? *Cell.* **115:** 377–388.
35. Pike, L. J. 2003. Lipid rafts: bringing order to chaos. *J. Lipid Res.* **44:** 655–667.
36. Kay, J. G., R. Z. Murray, J. K. Pagan, and J. L. Stow. 2006. Cytokine secretion via cholesterol rich lipid raft associated SNAREs at the phagocytic cup. *J. Biol. Chem.* **281:** 11949–11954.
37. Landry, Y. D., M. Denis, S. Nandi, S. Bell, A. M. Vaughan, and X. Zha. 2006. ABCA1 expression disrupts raft membrane microdomains through its ATPase-related functions. *J. Biol. Chem.* In press.
38. Li, Y., R. F. Schwabe, T. D. Vries-Seimon, P. M. Yao, M-C. Gerbod-Giannone, A. R. Tall, R. J. Davis, R. Flavell, D. A. Brenner, and I. Tabas. 2005. Free cholesterol-loaded macrophages are an abundant source of tumor necrosis factor-α and interleukin-6. *J. Biol. Chem.* **280:** 21763–21772.
39. Francone, O. L., L. Royer, G. Boucher, M. Haghpassand, A. Freeman, D. Brees, and R. J. Aiello. 2005. Increased cholesterol deposition, expression of scavenger receptors, and response to chemotactic factors in Abca1-deficient macrophages. *Arterioscler. Thromb. Vasc. Biol.* **25:** 1198–1205.
40. Wang, Y., and J. F. Oram. 2002. Unsaturated fatty acids inhibit cholesterol efflux from macrophages by increasing degradation of ATP-binding cassette transporter A1. *J. Biol. Chem.* **277:** 5692–5697.
41. Wang, Y., and J. F. Oram. 2005. Unsaturated fatty acids phosphorylate and destabilize ABCA1 through a phospholipase D2 pathway. *J. Biol. Chem.* **280:** 35896–35903.

Role of LCAT in HDL remodeling: investigation of LCAT deficiency states

Bela F. Asztalos,[1,*] Ernst J. Schaefer,[*] Katalin V. Horvath,[*] Shizuya Yamashita,[†] Michael Miller,[§] Guido Franceschini,[**] and Laura Calabresi[**]

Lipid Metabolism Laboratory,[*] Jean Mayer US Department of Agriculture Human Nutrition Research Center on Aging at Tufts University, Boston, MA; Department of Internal Medicine and Molecular Science,[†] Osaka University, Suita, Japan; Department of Medicine,[§] University of Maryland, Baltimore, MD; and Center E Grossi Paoletti, Department of Pharmacological Sciences,[**] University of Milan, Milan, Italy

Abstract To better understand the role of LCAT in HDL metabolism, we compared HDL subpopulations in subjects with homozygous (n = 11) and heterozygous (n = 11) LCAT deficiency with controls (n = 22). Distribution and concentrations of apolipoprotein A-I (apoA-I)-, apoA-II-, apoA-IV-, apoC-I-, apoC-III-, and apoE-containing HDL subpopulations were assessed. Compared with controls, homozygotes and heterozygotes had lower LCAT masses (−77% and −13%), and LCAT activities (−99% and −39%), respectively. In homozygotes, the majority of apoA-I was found in small, disc-shaped, poorly lipidated preβ-1 and α-4 HDL particles, and some apoA-I was found in larger, lipid-poor, discoidal HDL particles with α-mobility. No apoC-I-containing HDL was noted, and all apoA-II and apoC-III was detected in lipid-poor, preβ-mobility particles. ApoE-containing particles were more disperse than normal. ApoA-IV-containing particles were normal. Heterozygotes had profiles similar to controls, except that apoC-III was found only in small HDL with preβ-mobility. Our data are consistent with the concepts that LCAT activity: *1*) is essential for developing large, spherical, apoA-I-containing HDL and for the formation of normal-sized apoC-I and apoC-III HDL; and *2*) has little affect on the conversion of preβ-1 into α-4 HDL, only slight effects on apoE HDL, and no effect on apoA-IV HDL particles.—Asztalos, B. F., E. J. Schaefer, K. V. Horvath, S. Yamashita, M. Miller, G. Franceschini, and L. Calabresi. **Role of LCAT in HDL remodeling: investigation of LCAT deficiency states.** ***J. Lipid Res.*** **2007.** 48: **592–599.**

Supplementary key words HDL subpopulations • apolipoproteins • reverse cholesterol transport

LCAT is a 416 amino acid protein that binds to lipoproteins or is present in lipid-free form in plasma and is secreted by the liver in humans (1). LCAT synthesizes the majority of cholesteryl esters in plasma by transferring a fatty acid from lecithin (phosphatidyl choline) to the 3-hydroxyl group of cholesterol. It is generally believed that LCAT maintains the unesterified cholesterol gradient between peripheral cells and HDL. Efflux of free cholesterol (FC) from cells occurs by a passive diffusion of FC between cellular membranes and acceptors and by mechanisms facilitated by scavenger receptor type B-I (SR-BI) and ABCs. In the presence of LCAT, the bi-directional movement of cholesterol between cells and HDL results in net cholesterol efflux (2, 3). Therefore, LCAT plays a central role in the initial steps of reverse cholesterol transport. LCAT is activated primarily by apolipoprotein A-I (apoA-I), but can also be activated by apoA-IV, apoC-I, and apoE (4, 5). Both the binding and activation of LCAT on the surface of HDL are essential for esterification of FC and accumulation of cholesteryl esters in the core of HDL.

Familial LCAT deficiency (FLD) is characterized by the absence of LCAT activity and reduced HDL cholesterol (HDL-C) level in plasma. In affected individuals, LCAT is either absent or present but inactive in plasma (6). LCAT has two distinct substrates: HDL and LDL. LCAT activity on HDL is called α-activity, and LCAT activity on LDL is called β-activity (7, 8). Lack of α-LCAT activity causes fish eye disease (FED). Homozygous subjects with FLD have corneal opacification, anemia, proteinuria, hematuria, and ultimately, renal failure, often requiring kidney transplantation (9). FED subjects have no clinical manifestation other than an age-dependent corneal opacification. Although it is not clear whether LCAT deficiency is directly linked to premature coronary artery disease (CAD), increased risk for CAD has been reported in some patients (9). Data obtained from cholesterol-fed human-LCAT transgenic rabbits indicated that HDL-C increased

Manuscript received 12 September 2006 and in revised form 19 October 2006 and in re-revised form 29 November 2006.

Published, JLR Papers in Press, December 20, 2006.
DOI 10.1194/jlr.M600403-JLR200

Abbreviations: apoA-I, apolipoprotein A-I; CAD, coronary artery disease; CETP, cholesteryl ester transfer protein; EL, endothelial lipase; FC, free cholesterol; FED, fish eye disease; FLD, familial LCAT deficiency; HDL-C, HDL cholesterol; sPLA2, secretory phospholipase A2; SR-BI, scavenger receptor type B-I; TG, triglyceride.

[1]To whom correspondence should be addressed.
e-mail: bela.asztalos@tufts.edu

due to decreased catabolism of larger HDL particles, suggesting that the size of HDL may modulate the selective HDL-C uptake by the liver (10). In human-LCAT transgenic mice, the liver uptake of HDL was reduced by 41%, resulting in a substantial increase of large HDL particles that might be atherogenic (11) due to the fact that mice lack cholesteryl ester transfer protein (CETP) and that continued increase of cholesteryl ester in HDL by high levels of LCAT changes both the size and lipid composition of HDL. When CETP was coexpressed in LCAT transgenic mice, HDL size and composition changed and the animals were protected from atherosclerosis (12). These data suggest that under normal conditions in which CETP is present as in humans, increased LCAT activity is likely to increase HDL cholesterol and size and might reduce the risk for atherosclerosis. Our previous data suggest that the two largest, spherical, cholesteryl ester-rich HDL particles, α-1 and α-2, are good substrates for SR-BI in a human hepatoma cell line (13).

Our aim was to gain insight into the role that LCAT plays in HDL metabolism as well as to better understand LCAT deficiency states. We have examined apoA-I-, -A-II-, -A-IV-, -C-I-, -C-III-, and -E-containing HDL subpopulation profiles in LCAT-deficient homozygotes and heterozygotes and in control subjects. The data we present indicate that LCAT plays a very significant role in HDL particle metabolism, composition, and remodeling.

MATERIALS AND METHODS

Subjects

We examined plasma obtained from 11 homozygous LCAT-deficient subjects of Italian (n = 7), Japanese (n = 3), and US (n = 1) origin, as well as from 11 heterozygous LCAT-deficient subjects from Italy. Plasma obtained from gender-matched control subjects from the US (n = 15), Italy (n = 4), and Japan (n = 3) was used in this comparison. Homozygous and heterozygous subjects from Italy have been described previously (14). All homozygous subjects had primary hypoalphalipoproteinemia as defined by a plasma HDL-C level below the 5th percentile for the age- and gender-matched general populations of the specific countries. One homozygous subject from Japan had FED; however, none of the measured parameters of this subject were different by more than 1 SD from those of the other 10 homozygotes.

Sample handling and measurements

Blood was collected from all subjects after an overnight fast and immediately placed on ice. Plasma was separated by low-speed centrifugation at 4°C and was stored at −°80 C until use. Samples were sent to the Lipid Metabolism Laboratory at Tufts University on dry ice and were thawed in a 37°C water bath for 1–2 min and then placed on ice just before use. Plasma total cholesterol, HDL-C, and triglyceride (TG) levels were determined using standard enzymatic techniques. Plasma concentrations of apoA-I, -A-II, and -B were determined by immunoturbidimetry. Plasma concentrations of apoA-IV, -C-I, -C-III, and -E were estimated by dot-blot analyses and expressed as arbitrary units. LCAT gene analyses, activity, and mass measurements were performed as described previously (14). HDL subpopulations were determined by nondenaturing two-dimensional PAGE, immunoblotting, and image analysis as described previously (15). Four microliters of plasma was applied and electrophoresed on a vertical-slab agarose gel (0.7%) in the first dimension at 250 V until the α-mobility front moved 3.5 cm from the origin. The agarose gel was sliced, and the strips were applied onto 3–35% nondenaturing concave gradient polyacrylamide gels. In the second dimension, gels were electrophoresed to completion at 250 V for 24 h at 10°C, followed by electrotransfer to nitrocellulose membranes at 30 V for 24 h at 10°C. The specific apolipoproteins were immuno-localized on the membrane with mono-specific goat anti-human primary and ^{125}I-labeled secondary antibodies [immunopurified rabbit F(ab')$_2$ fraction against goat IgG]. The bound ^{125}I-labeled secondary antibody was quantified in a FluoroImager (Molecular Dynamics). Each membrane was first probed for the apolipoprotein of primary interest and than reprobed for apoA-I for reference.

Data analysis

Means and standard deviations were calculated for all study groups. Data obtained from homozygotes and heterozygotes were compared with data from controls using ANOVA analyses. A two-tailed $P < 0.05$ was considered as significant.

RESULTS

Table 1 shows data on LCAT mass and activity as well as on lipids and apolipoproteins in controls (n = 22), heterozygotes (n = 11), and homozygotes (n = 11) for LCAT deficiency. Heterozygotes had 39% of the LCAT activity and 87% of the LCAT mass of controls. They had lower apoA-I (−22%), apoA-II (−19%), HDL-C (−15%), and

TABLE 1. Characteristics of study participants

	Controls (n = 22)	Heterozygotes (n = 11)	Homozygotes (n = 11)
Male/female	17/5	7/4	10/1
LCAT mass (μg/ml)	4.60 ± 1.01	4.02 ± 1.07	1.04 ± 0.96*
LCAT activity (nmol/ml/h)	33.0 ± 18.1	20.21 ± 1.6*	0.44 ± 0.66*
Total cholesterol (mg/dl)	200 ± 38	171 ± 37*	112 ± 63*
LDL-C (mg/dl)	126 ± 33	99 ± 33*	65 ± 54*
HDL-C (mg/dl)	54 ± 13	46 ± 12*	9 ± 5*
TG (mg/dl)	137 ± 88	127 ± 45	203 ± 146*
apoA-I (mg/dl)	140 ± 25	109 ± 17*	34 ± 11*
apoA-II (mg/dl)	38 ± 4	31 ± 5	11 ± 6*
apoB (mg/dl)	96 ± 16	97 ± 25	31 ± 17*

ApoA-I, apolipoprotein A-I; HDL-C, HDL cholesterol; TG, triglyceride. Data are mean ± SD.
* Significantly different ($P < 0.05$) from controls.

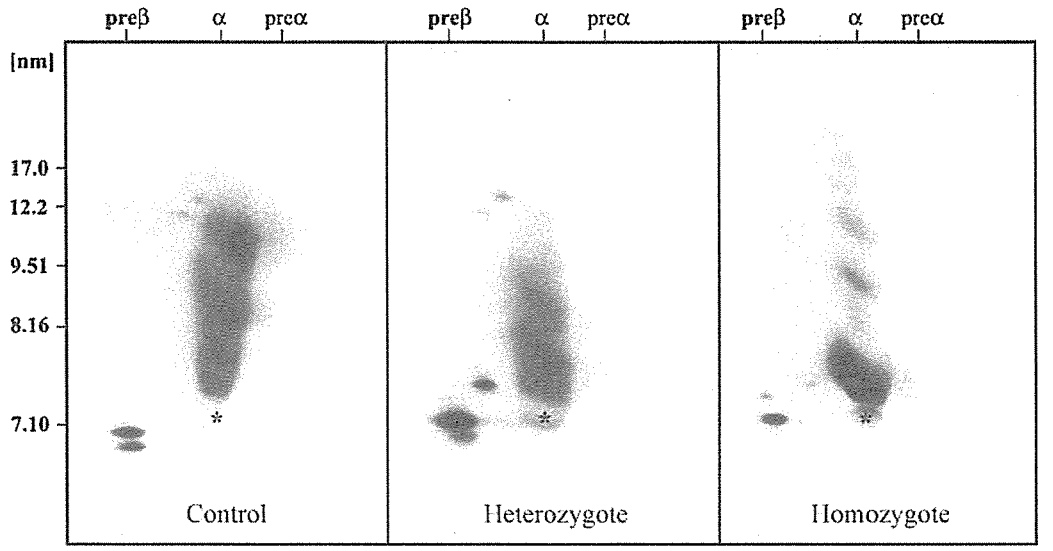

Fig. 1. Apolipoprotein A-I (apoA-I)-containing HDL subpopulations of representative control, heterozygous, and homozygous LCAT-deficient subjects separated by two-dimensional, nondenaturing agarose-PAGE. The asterisk represents the endogenous human serum albumin marking the α-mobility front.

TG (−7%) values compared with controls. Homozygotes had about 1% of the LCAT activity and about 23% of the LCAT mass of controls. They had significantly lower HDL-C (−83%), apoA-I (−76%), apoA-II (−71%), apoB (−68%), and LDL-C (−49%), and 48% higher TG values than controls.

Figure 1 and **Table 2** summarize data on apoA-I-containing HDL subpopulations in controls and in heterozygous and homozygous LCAT-deficient subjects. Heterozygotes had one extra particle in the preβ-1 region (preβ-1×); however, all of their other apoA-I-containing HDL subpopulations were comparable to controls in electrophoretic mobility and size. ApoA-I distribution in heterozygotes was shifted toward the smaller HDL particles: there was a 2-fold increase in preβ-1 level, a 23% increase in α-4, and a 45% increase in preα-4 levels compared with controls. There were significant decreases in the concentrations of all the other HDL particles, whereas the mean concentration of α-3, an intermediate-sized particle, was similar to that of controls. In homozygotes, the majority of apoA-I was detected in small, lipid-poor, disc-shaped HDL particles (preβ-1 and α-4). Despite the low plasma concentrations of apoA-I in homozygous subjects, the apoA-I concentrations of these particles were comparable to those of controls. We have also observed larger (~8 nm–20 nm) apoA-I-containing HDL particles with α-mobility in many of the homozygotes. **Figure 2** represents the distribution of apoA-II-containing particles—superimposed on apoA-I-containing particles—in representative control, heterozygous, and homozygous LCAT-deficient subjects. In control subjects, α-2 and α-3 HDL contain apoA-I and apoA-II. In heterozygotes, some apoA-II was detected in the preβ-1 region but the majority of apoA-II was distributed in the α-2 and α-3 subpopulations, with a slight shift toward the smaller α-3 particles, compared with controls. In contrast to controls, homozygotes had a very low level of apoA-II, which was detected in a small, lipid-poor particle, comigrating with the regular LpA-I preβ-1 HDL particles. Total or partial LCAT deficiency had no significant effect on the concentration of apoA-IV or the distribution of apoA-IV-containing HDL particles (**Fig. 3**). There were no significant differences between heterozygotes and controls in apoC-I concentration and distribution (**Fig. 4**). In contrast, homozygotes had significantly lower apoC-I levels, and their apoC-I was found on the top of the gel with β-mobility, indicating that apoC-I was present solely in VLDL particles, not in α-mobility HDL particles, as in controls and heterozygotes. The concentrations and distribution of apoC-III were significantly different between LCAT-deficient subjects and controls (**Fig. 5**). In controls, the majority of apoC-III comigrated with apoA-I in α-1 and α-2 HDL, and some was also found

TABLE 2. Concentrations of HDL subpopulations as determined by apoA-I content

	Controls (n = 22)	Heterozygotes (n = 11)	Homozygotes (n = 11)
Preβ-1_x	Not detectable	0.7 ± 0.9*	1.6 ± 1.0*
Preβ-1_a	8.2 ± 3.2	14.6 ± 5.4*	7.9 ± 4.0
Preβ-1_b	4.1 ± 1.6	10.3 ± 8.1*	1.8 ± 1.1*
Preβ-2_a	0.7 ± 0.4	0.3 ± 0.2*	Not detectable
Preβ-2_b	1.0 ± 0.5	0.5 ± 0.3*	Not detectable
Preβ-2_c	0.5 ± 0.3	0.2 ± 0.2*	Not detectable
α-1	16.7 ± 8.9	11.0 ± 8.6*	
α-2	39.1 ± 9.6	25.3 ± 6.7*	11.6 ± 2.4
α-3	24.3 ± 5.6	23.2 ± 5.5	
α-4	13.4 ± 3.6	16.5 ± 3.5*	12.1 ± 7.0
Preα-1	5.2 ± 3.3	0.9 ± 0.9*	
Preα-2	6.2 ± 2.4	1.9 ± 1.1*	0.6 ± 0.4
Preα-3	3.4 ± 1.4	2.0 ± 1.0*	
Preα-4	1.1 ± 0.4	1.6 ± 0.8*	0.6 ± 1.0

Data are mean (mg/dl) ± SD.
*Significantly different ($P < 0.05$) from control.

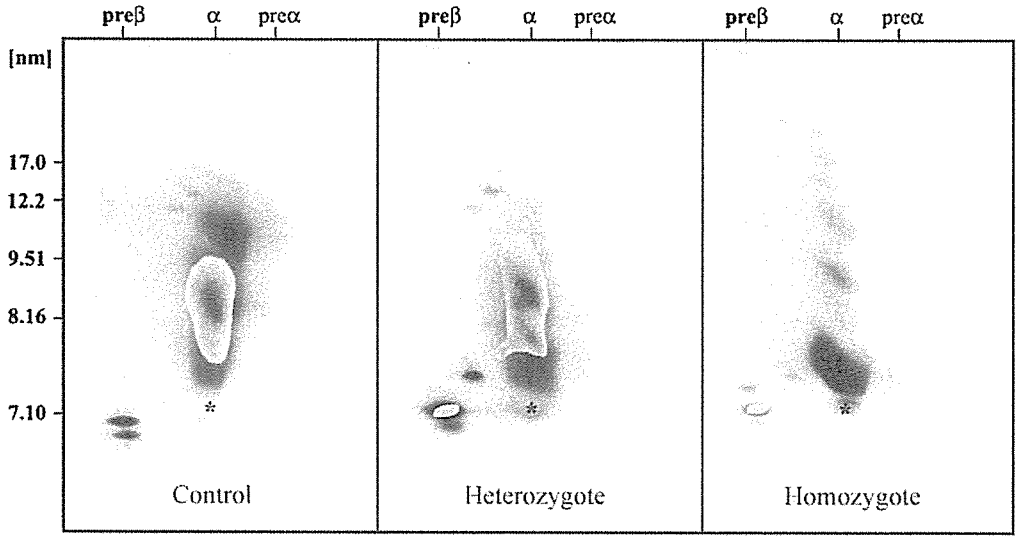

Fig. 2. ApoA-II-containing HDL subpopulations of representative control, heterozygous, and homozygous LCAT-deficient subjects superimposed on the image of apoA-I-containing subpopulations. LCAT-deficient subjects have apoA-II in small, preβ-migrating HDL particles. The asterisk represents the endogenous human serum albumin marking the α-mobility front.

in the α-3 and α-4 size range, with no comigration with apoA-I. In contrast, practically all of the apoC-III was detected in small, lipid-poor HDL particles in homozygotes and heterozygotes. ApoE-containing particles migrated with β-preβ-mobility in the size range between 12 nm and VLDL size, with a median diameter of 16.5 nm in controls (**Fig. 6**) and no overlap with apoA-I-containing HDL particles. In heterozygotes, apoE was also found in large β-preβ-mobility particles, with no comigration with apoA-I. Interestingly, the size of apoE-containing particles was somewhat increased in heterozygotes compared with controls. Homozygotes had much less apoE than controls. ApoE concentrations in the larger particles decreased, and smaller apoE-containing particles appeared in the plasma of homozygotes.

DISCUSSION

The purpose of this study was to gain insight into the role that LCAT plays in HDL metabolism as well as to better understand LCAT deficiency states. Characteriz-

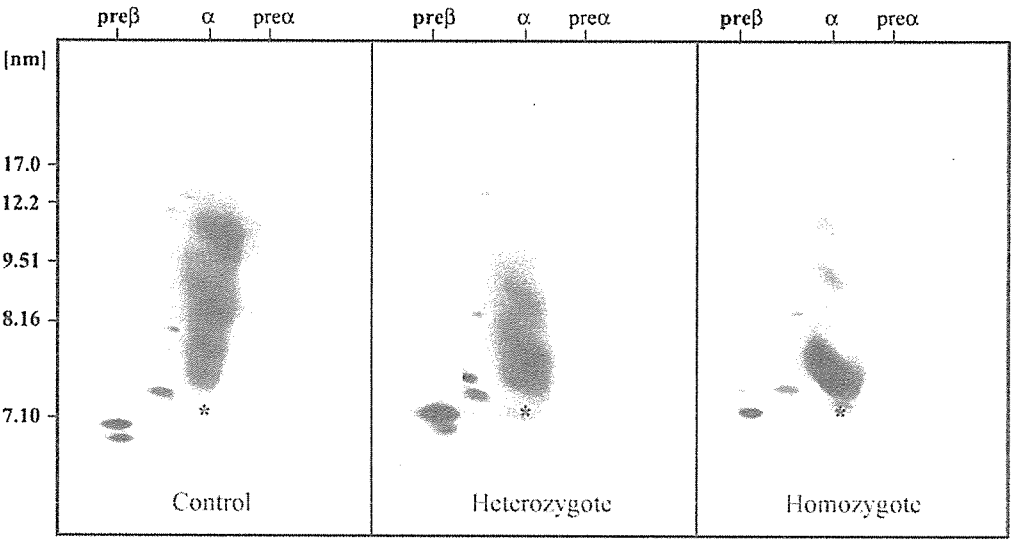

Fig. 3. ApoA-IV-containing HDL subpopulations of representative control, heterozygous, and homozygous LCAT-deficient subjects superimposed on the image of apoA-I-containing subpopulations. Total or partial LCAT deficiency has no significant effect on the distribution of apoA-IV-containing HDL particles. The asterisk represents the endogenous human serum albumin marking the α-mobility front.

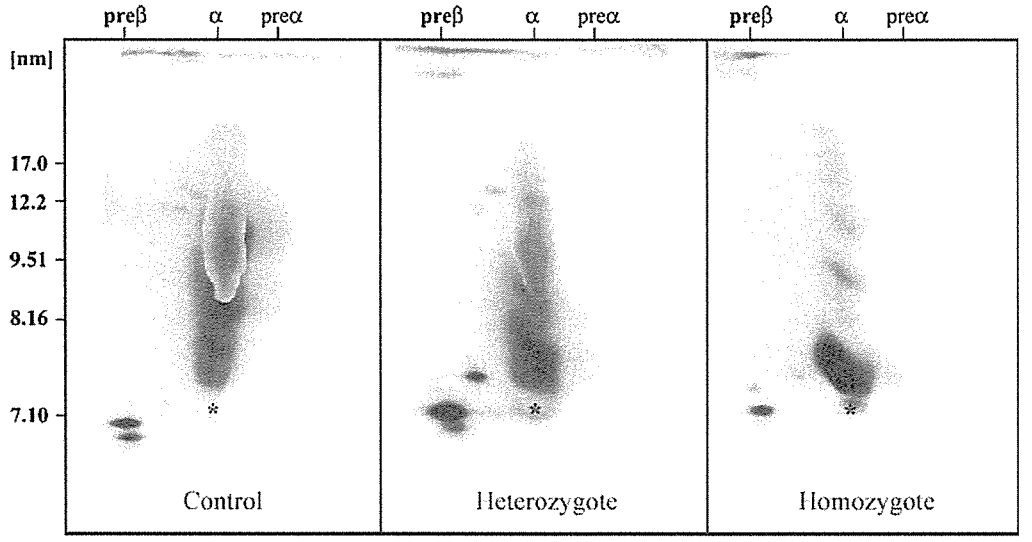

Fig. 4. ApoC-I-containing HDL subpopulations of representative control, heterozygous, and homozygous LCAT-deficient subjects superimposed on the image of apoA-I-containing subpopulations. In homozygotes, apoC-I has only been detected on the top of the gel with β-mobility (VLDL) in contrast to controls and heterozygotes. The asterisk represents the endogenous human serum albumin marking the α-mobility front.

ing HDL particles in patients with rare inborn errors of HDL metabolism has been helpful in better understanding HDL particle metabolism and reverse cholesterol transport. We have documented that Tangier disease patients had: *1*) apoA-I only in the preβ-1 HDL particles, 2) no apoA-II-containing HDL, and *3*) decreased size of apoE HDL. ApoA-IV was not significantly influenced by the lack of ABCA1-mediated cellular cholesterol efflux (16). We have subsequently reported that HDL subpopulations in CETP-deficient homozygotes were very large, compositionally undifferentiated HDL particles (17). Therefore, CETP activity is essential for the formation of distinguished HDL particles in the normal size range of HDL. Most importantly, CETP activity is essential for the formation of discrete LpA-I, LpA-I:A-II, and LpE HDL particles.

In the present manuscript, we document the role of LCAT in HDL metabolism and remodeling in plasma. The first important observation is that LCAT activity is not

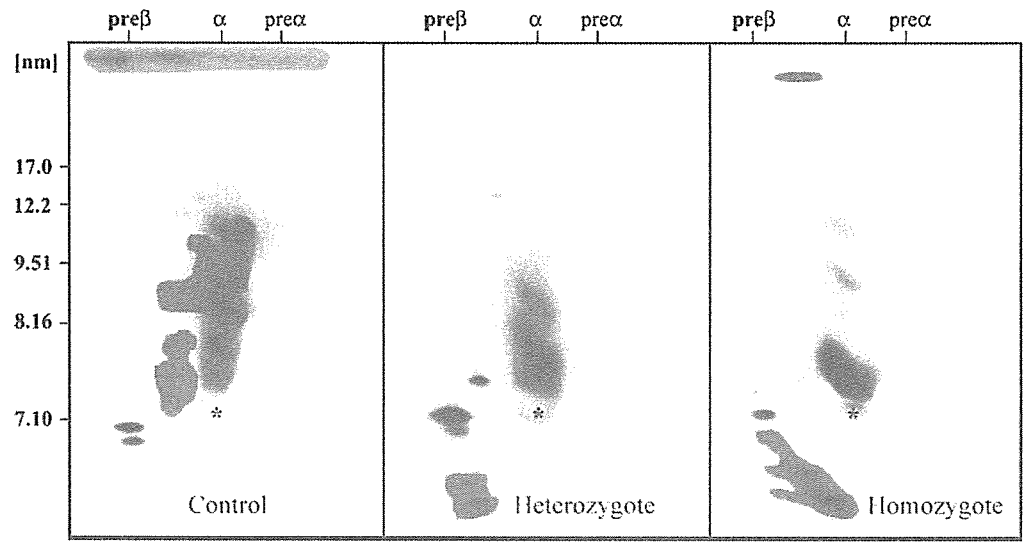

Fig. 5. ApoC-III-containing HDL subpopulations of representative control, heterozygous, and homozygous LCAT-deficient subjects superimposed on the image of apoA-I-containing subpopulations. In controls, the majority of apoC-III comigrates with apoA-I in α-1 and α-2 HDL, and some has also been found in the α-3 and α-4 size range with no comigration with apoA-I. In homozygotes and heterozygotes, practically all apoC-III has been detected in small, lipid-poor HDL particles. The asterisk represents the endogenous human serum albumin marking the α-mobility front.

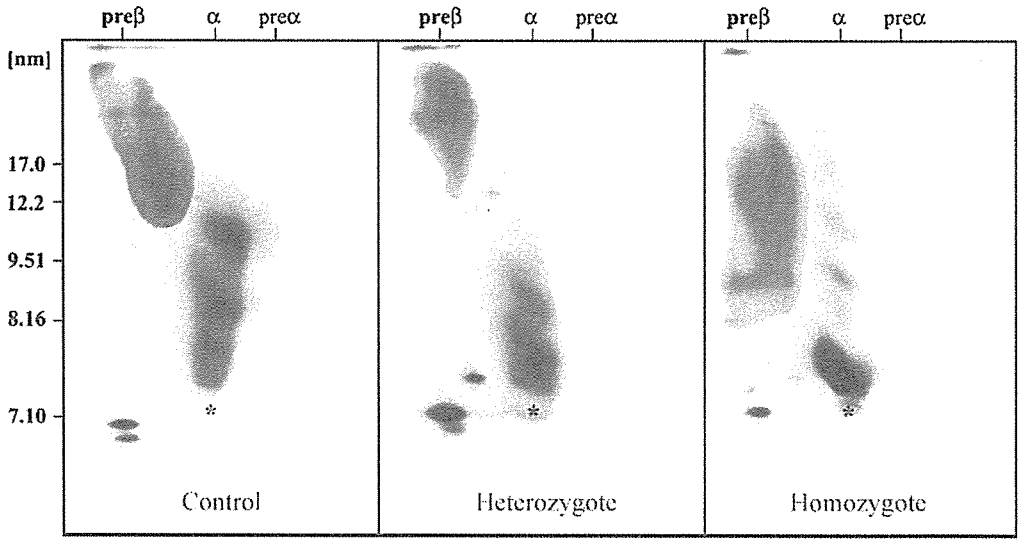

Fig. 6. ApoE-containing HDL subpopulations of representative control, heterozygous, and homozygous LCAT-deficient subjects superimposed on the image of apoA-I-containing subpopulations. There is no comigration of apoE- and apoA-I-containing particles. The asterisk represents the endogenous human serum albumin marking the α-mobility front.

necessary for the transformation of preβ-1 HDL into α-mobility HDL. Preβ-1 binds to ABCA1 and removes phospholipids and unesterified cholesterol from cells (13). During this process, there are probably changes in apoA-I conformation and electrophoretic charge. We hypothesize that α-4 HDL contains two molecules of apoA-I, as is the case for preβ-1 HDL. Larger (~8 nm–20 nm) α-mobility HDL particles have also been observed in many of the homozygotes. The tight bands of these particles suggest that these are poorly lipidated, discoidal HDL aggregates. We have no data indicating whether LCAT can act on these large, stacked disks or can use only the small α-4 HDL as a substrate. The apoA-I-containing HDL subpopulation profile of heterozygotes resembles that of low HDL-C CAD patients, inasmuch as apoA-I distribution is shifted toward the smaller particles. ApoA-II is dramatically reduced in homozygous subjects, probably because of fast catabolism (18), and, interestingly, it comigrates with preβ-1 HDLs, which normally contain only apoA-I. Some apoA-II also comigrates with preβ-1 HDL in heterozygotes; however, we do not know whether apoA-I and apoA-II are in the same particles. As a result of the presence of cholesteryl ester in the core of HDL particles, apoA-II binds to α-2 and α-3 HDL particles very early, as indicated in heterozygotes whose apoA-I/apoA-II ratios are increased in these particles. Our data also suggest that LCAT is not a key player in the formation of apoA-IV-containing particles. On the basis of these and other findings (16, 17), we hypothesize that the metabolism of apoA-IV-containing particles is independent of ABCA-1-mediated cellular cholesterol efflux, as well as of CETP and LCAT activities in humans. The majority of apoC-I comigrates with apoA-I-containing α-1 HDL in controls. About 20% of apoC-I in controls and ~35% of apoC-I in heterozygotes have α-mobility with larger than α-1 size. Homozygotes have apoC-I only in the VLDL fraction, indicating that the neutral lipid core is essential for the incorporation of apoC-I into HDL. ApoC-III has a complex pattern in controls: ~25% of apoC-III comigrates with α-1, ~50% comigrates with α-2, ~15% is found in VLDL, and the rest is in the HDL size range but does not overlap with apoA-I-containing particles. Interestingly, in both affected groups, apoC-III has been detected in small, lipid-poor form (free apoC-III), indicating that apoC-III is probably sensitive to the lipid and apolipoprotein composition of HDL. The large amount of free apoC-III in affected subjects also indicates that the fractional catabolic rate of this apolipoprotein is not increased with decreased particle size, which is clearly not the case for apoA-I and apoA-II. We clearly demonstrate that apoE-containing particles do not overlap with apoA-I-containing particles either in controls or in LCAT-deficient subjects in this study. [We have only seen apoE comigrating with apoA-I in homozygous CETP-deficient subjects where HDL size reached the size of LDL and the particles were probably loaded with excess amounts of cholesteryl ester (17)]. Although apoA-I concentrations were significantly lower in the large particles in heterozygous LCAT-deficient subjects, apoE concentrations were significantly increased in the large apoE HDL particles in these subjects. We have no explanation for this phenomenon. We do not know the chemical composition of these particles. In homozygous LCAT-deficient subjects, we observed only slightly more apoE in apparently lipid-poor particles. Therefore, LCAT activity does not seem to be a key player in supplying neutral lipids for apoE-containing HDL. Alternatively, TGs seem to be sufficient for the formation of the core of apoE HDL in homozygotes. If this is true, the questions arise as to how this TG-rich apoE HDL is metabolized and what its role in lipoprotein metabolism and CAD risk is.